from the first tumor excision to reconstruction, including the assessment of the frozen section, was 124 min. No local recurrences have been reported to date, after a median follow-up of 14.9 months (range: 1–48 months) (Table II). As shown in Figure 3, SCC on the lower lip who underwent complete histological margin control was reconstructed with combination of local flap.

DISCUSSION

Although MMS is the most useful surgical method for high-risk skin cancer in USA and European countries, it is generally performed only under local anesthesia by experienced Mohs surgeons and technicians [5]. However, some cases of large and deep defect require reconstruction under general anesthesia. In these cases, reconstructive surgery should be planned not on the same day of the resection. In contrast, intraoperative histological evaluation is frequently performed in many institutions at which it is difficult to perform a complete MMS procedure due to health insurance and other reasons [7]. Intraoperative histological evaluation is especially common for surgery under general anesthesia in which resection and reconstruction are completed together [8]. To save time and increase the accuracy of histological analysis for surgical margins, it is easier and more convenient to add an essential technique of MMS to conventional intraoperative histological evaluation than to introduce a new MMS system itself from the beginning. The technical simplicity of this procedure allows it be used by non-MMS surgeons in the treatment of non-melanoma patient at most institutions.

Micrographic surgery in which complete histological visualization and evaluation of surgical margins, is used to detect unseen tumor outgrowth [9]. In addition to the traditional Mohs micrographic surgery, many variations of this histopathological approach for surgery have been developed and described in the literature [10]. Although the approach differs for each variation, methods are categorized as those that use a frozen section versus using a permanent section [11,12], and those that evaluate the peripheral margin only versus including the deep margin [13].

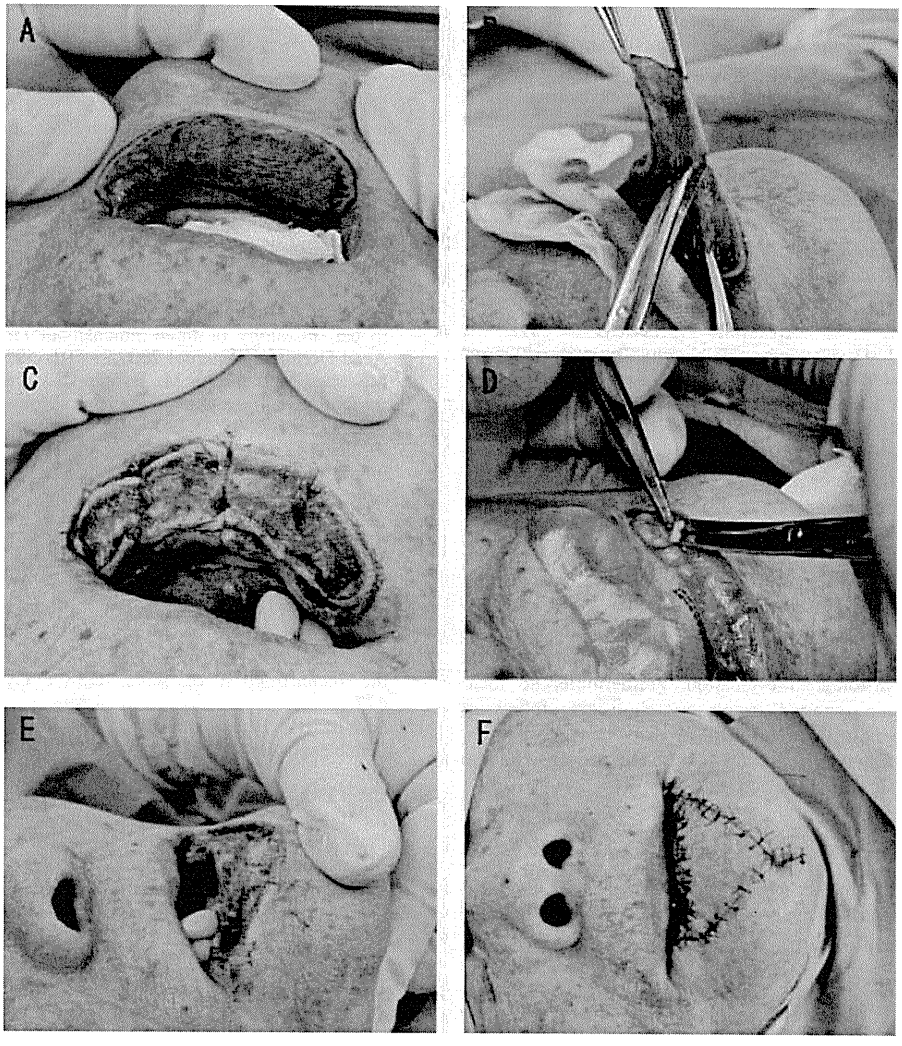

Fig. 3. A 79-year-old woman with SCC on the lower lip who underwent complete histological margin control by frozen section (case 15 in Table I and II). **A**: The initial surgical margin is 2 mm (solid line) from the clinical border (dotted line). **B**: After parallel excision by DBS, the central tumor can be easily resected along the inner line. **C**: After excision of the tumor, the defect is sub-sectioned into four regions. **D**: Each piece is excised easily in uniform width of skin. **E**: The final defect after complete excision of tissue under histological evaluation by frozen section. **F**: Double V-Y advancement flap and mucous transposition flap from the right cheek are used to reconstruct the lower lip.

A basic element of our procedure is resection of the whole tumor followed by concurrent excision of an additional outer layer for complete histological evaluation of the excision margins in three dimensions. That element involves completing the first two steps of MMS together by using permanent sections for histological evaluation of the tumor and using the frozen section only in re-excision of specimens of an additional outer layer from the tumor defect. Our system requires fewer frozen tissue sections to be processed than for MMS. There is a definite difference in total procedure time between our procedure and MMS. In our procedure, a number of each process for making frozen section has to limit in once or twice. Therefore, one distinguishing feature our procedure is the detection and removal of subclinical irregular invasions of tumor cells rather than aesthetic preservation through maximum tissue conservation.

To improve the efficiency of our procedure, an additional layer should excised correctly after gross tumor resection, and this layer should include skin with uniform width for ease in preparing frozen sections. Thus, the distance between the double blades is set at 2 mm. Minor successive improvements to the scalpel holder allow a parallel excision line to be made in a single motion. The greatest advantage of the DBS over the single blade is that it makes it easier for the surgeon to harvest tissue strips of uniform width. The uniform strips are more easily processed for frozen section evaluation, which increases the efficiency of the total intraoperative procedure time and the accuracy of histological analysis for surgical margins.

The DBS consists of a handle with two parallel scalpel blades that may be set at variable widths by adjusting metal spacers. The concept of this device was described in 1977 by Coiffman [14] and the device was originally created to harvest donor strips for hair transplantation. The DBS has been described with respect to the removal of surgical scars [15], BCCs [16], non-melanoma skin cancers [17] and dermatosarcoma protuberans [18]. A few articles detail the potential advantages of the DBS in micrographic surgery [18]. However previous reports describe methods using DBS only for peripheral margin evaluation or for staged margin evaluation, and not for true MMS procedures [18].

There is the concern that the procedure will increase the time required to complete tumor removal, compared to conventional intraoperative histological evaluation. However, 60% of our procedures required only one re-excison for complete histologic margin control. Complete surgical margin negative required only two re-excisions in total. The median procedure time was 107 min to clear the surgical margin with one re-excision and 149 min to clear it with two re-excisions. These procedure times would not differ significantly from those for patients undergoing conventional surgical excision with intraoperative histological evaluation. Furthermore, no local recurrences have been reported in on our short-term follow-up (14.9 months). We believe that the reliability of our method is high, although long-term follow-up data are required to substantiate the effectiveness of this surgical approach.

CONCLUSION

In conclusion, DBS may be used as an alternative for complete histological margin control at many hospitals where complete MMS is not available, especially in Asia. This method appears to be time-saving and easy to apply with existing systems. It is convenient and may require fewer excisions than with MMS.

REFERENCES

1. Karagas MR, Greenberg ER, Spencer SK, et al.: Increase in incidence rates of basal cell and squamous cell skin cancer in New Hampshire, USA. New Hampshire Skin Cancer Study Group. Int J Cancer 1999;81:555–559.
2. Neville JA, Welch E, Leffell DJ: Management of nonmelanoma skin cancer in 2007. Nat Clin Pract Oncol 2007;4:462–469.
3. Batra RS, Kelley LC: A risk scale for predicting extensive subclinical spread of nonmelanoma skin cancer. Dermatol Surg 2002;28:107–112.
4. Aoyagi S, Nouri K: Difference between pigmented and non-pigmented basal cell carcinoma treated with Mohs micrographic surgery. Dermatol Surg 2006;32:1375–1379.
5. Brodland DG, Amonette R, Hanke CW, et al.: The history and evolution of Mohs micrographic surgery. Dermatol Surg 2000; 26:303–307.
6. Takenouchi T, Nomoto S, Ito M: Factors influencing the linear depth of invasion of primary basal cell carcinoma. Dermatol Surg 2001;27:393–396.
7. Ghauri RR, Gunter AA, Weber RA: Frozen section analysis in the management of skin cancers. Ann Plast Surg 1999;43:156–160.
8. Gandour-Edwards RF, Donald PJ, Wiese DA: Accuracy of intraoperative frozen section diagnosis in head and neck surgery: Experience at a university medical center. Head Neck 1993; 15:33–38.
9. Mohs FE: Chemosurgery: Microscopically controlled surgery for skin cancer–past, present and future. J Dermatol Surg Oncol 1978;4:41–54.
10. Moehrle M, Breuninger H, Röcken M: A confusing world: What to call histology of three-dimensional tumour margins? J Eur Acad Dermatol Venereol 2007;21:591–595.
11. Mahoney MH, Joseph M, Temple CL: The perimeter technique for lentigo maligna: An alternative to Mohs micrographic surgery. J Surg Oncol 2005;91:120–125.
12. Möller MG, Pappas-Politis E, Zager JS, et al.: Surgical management of melanoma-in-situ using a staged marginal and central excision technique. Ann Surg Oncol 2009;16:1526–1536.
13. Moehrle M, Dietz K, Garbe C, et al.: Conventional histology vs. three-dimensional histology in lentigo maligna melanoma. Br J Dermatol 2006;154:453–459.
14. Coiffman F: Use of square scalp grafts for male pattern baldness. Plast Reconstr Surg 1977;60:228–232.
15. Bowen ML, Charnock FM: The Bowen double-bladed scalpel for the reconstruction of scars. Obstet Gynecol 1994;83:476–477.
16. Schultz BC, Roenigk HH, Jr.: The double scalpel and double punch excision of skin tumors. J Am Acad Dermatol 1982;7:495–499.
17. Chen TM, Wanitphakdeedecha R, Nguyen TH: Multibladed knife for staged surgical margin control in nonmelanoma skin cancer. Plast Reconstr Surg 2008;121:1870–1871.
18. Moossavi M, Alam M, Ratner D: Use of the double-bladed scalpel in peripheral margin control of dermatofibrosarcoma protuberans. Dermatol Surg 2000;26:599–601.

BJD
British Journal of Dermatology

Partially disturbed lamellar granule secretion in mild congenital ichthyosiform erythroderma with *ALOX12B* mutations

M. Akiyama, K. Sakai, T. Yanagi, N. Tabata,* M. Yamada† and H. Shimizu

Department of Dermatology, Hokkaido University Graduate School of Medicine, North 15 West 7, Kita-ku, Sapporo 060-8638, Japan
**Division of Dermatology and †Department of Pediatrics and Neonatal Intensive Care Unit, Japanese Red Cross Sendai Hospital, Sendai, Japan*

Correspondence
Masashi Akiyama.
E-mail: akiyama@med.hokudai.ac.jp

Accepted for publication
17 February 2010

Key words
ichthyosis, keratinization, lipid, lipoxygenase, LOX

Conflicts of interest
None declared.

DOI 10.1111/j.1365-2133.2010.09745.x

Congenital ichthyosiform erythroderma (CIE) (OMIM 242100) is a major type of autosomal recessive congenital ichthyosis (ARCI) showing generalized scaling and erythroderma without blister formation.[1] Mutations in *ALOX12B* (OMIM 603741), encoding 12R-lipoxygenase (LOX), were identified in patients with CIE in 2002.[2] To date, several *ALOX12B* mutations have been reported in CIE families.[3,4] LOXs are a family of nonhaem, iron-containing dioxygenases which catalyse dioxygenation of fatty acids with one or more (Z,Z)-1,4-pentadiene moieties.[5] Three members of the human LOX family, 15-LOX-2, 12R-LOX and eLOX-3, are preferentially expressed in the skin.[5,6] The 12R-LOX pathway leads to hepoxilin B3 and trioxilin B3[7] resulting in 20-carboxy-trioxilin A3,[5] which is thought to be a key biological regulator in the skin.[8] 12R-LOX deficiency results in a CIE phenotype in humans[2,9,10] and in mice.[11,12] We report that a Japanese patient with CIE, harbouring one previously unreported *ALOX12B* mutation p.Arg442Gln and another known mutation p.Arg432X, showed partially disturbed secretion of lamellar granule (LG) contents in the epidermis.

Case and methods

The patient was the first child of healthy, unrelated Japanese parents. There was no family history of any related disorders. The male child was born via uncomplicated, vaginal full-term delivery. The newborn was covered by a collodion membrane and showed thick scales on a background of erythroderma over his entire body, with skin fissures on the trunk (Fig. 1a–c). Moderate ectropion and eclabium were seen. Hands and feet were oedematous, and the palms and soles were involved. The patient was treated with a topical application of white petrolatum with an occlusive dressing technique in a humid incubator. The hyperkeratosis and oedema were remarkably reduced within 2 weeks. At age 3·5 months, the patient showed mild white to grey-coloured scales over the erythematous skin covering his entire body (Fig. 1d–f).

Mutation analysis of *ALOX12B* was performed using genomic DNA isolated from peripheral blood cells of the patient and his parents.

Results and discussion

Mutation analysis of *ALOX12B* revealed that the patient was a compound heterozygote for a known nonsense mutation p.Arg432X (c.1294C>T) in exon 10 and a previously unreported missense mutation p.Arg442Gln (c.1325C>T) in exon 10 (GenBank NM_001139.2) (Fig. 1g, h). The nonsense mutation p.Arg432X was present in a heterozygous fashion in his mother, although p.Arg442Gln was not found in the parents and was thought to be a *de novo* mutation. The mutations were verified by mutant allele-specific amplification analysis. No mutation was found in the sequence analysis of 200 alleles from 100 normal, unrelated Japanese individuals, and therefore it is unlikely to be a polymorphism (data not shown). No other pathogenic mutations were found in *TGM1* (OMIM 190195), *ABCA12* (OMIM 607800), *NIPAL4* (ichthyin; OMIM 609383), *CYP4F22* (previously known as *FLJ39501*; OMIM 611495) or *ALOXE3* (OMIM 607206) by direct sequencing analysis.

p.Arg432X results in a serious truncation of the 12R-LOX peptide, losing approximately half of the C-terminal catalytic LOX domain, and is thought to have a serious effect on the enzyme activity.

The arginine residue mutated by p.Arg442Gln is in the central part of the C-terminal catalytic LOX domain and is highly conserved among diverse species (Fig. 1i) and human LOX family members (Fig. 1i). These facts suggest that this arginine residue might be essential for enzyme activity and that the present missense mutation affects 12R-LOX activity.

Electron microscopy of a skin biopsy specimen from the trunk at age 6 days using ruthenium tetroxide postfixation revealed irregular-sized lipid droplets in the stratum corneum.

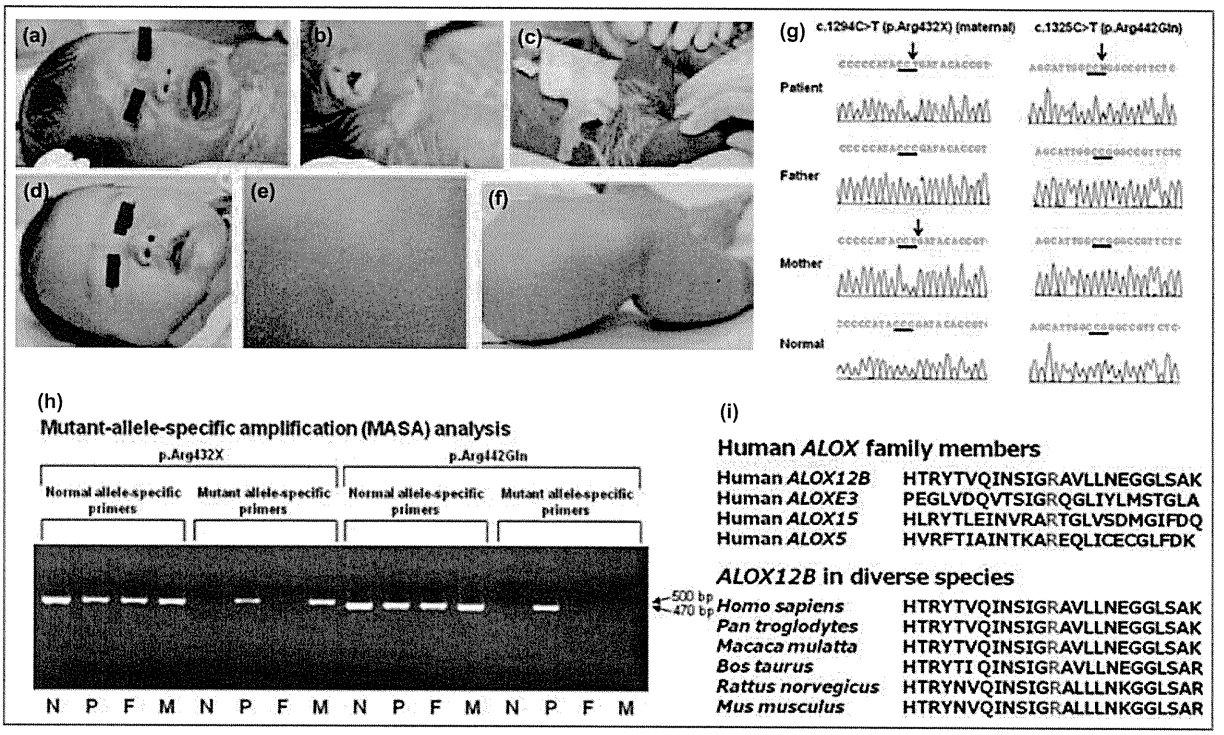

Fig 1. The patient's clinical features and compound heterozygous mutations in *ALOX12B*. (a–c) At 1 day of age: moderate ectropion and eclabium (a), a malformed auricle (b), and thick plate-like scales and fissures on the neck and the chest (b) and on the lower abdomen to the thigh (c). (d–f) At age 3·5 months: only slight, fine scales on the face (d), the back (e) and the thigh (f). (g) Compound heterozygous *ALOX12B* mutations, maternal p.Arg432X (c.1294C>T) and a novel missense mutation p.Arg442Gln (c.1325C>T) in exon 10 of the patient's genomic DNA. (h) Mutant allele-specific amplification (MASA) analysis showed a 500-bp band from p.Arg432X and a 470-bp band from p.Arg442Gln. N, normal; P, patient; F, father; M, mother. (i) Arginine 442 in 12R-lipoxygenase (LOX) altered by p.Arg442Gln; red character (R) is conserved among human *ALOX* family members (top) and diverse species (bottom).

Intact LGs were observed and intercellular lipid lamellae were seen in the intercellular space in the stratum corneum, although secretion of LG contents was disturbed in part in the granular layer cells (Fig. 2a–e).

Immunofluorescence staining revealed that one of the major basal keratins (keratin 5), differentiation-specific keratin (keratin 10) and ABCA12 were distributed normally in the basal layer, in the suprabasal layers, and in the granular layers, respectively, of the patient's epidermis (Fig. 2f, h, j). Immunoreactivity for cornified cell envelope-associated proteins involucrin, loricrin and transglutaminase 1 was seen normally distributed in the patient's upper epidermis (Fig. 2l, n, p).

Keratinocyte differentiation (keratinization)-specific molecules examined in the present study were normally distributed in the patient's epidermis. Also, keratinocyte differentiation defects were not morphologically or biochemically detected in *Alox12b*-disrupted mice.[11] These facts suggest that keratinocyte differentiation defects might not be involved in the pathogenesis of ichthyosis in CIE with *ALOX12B* mutations.

One report on ultrastructural features of the 12R-LOX-deficient human epidermis demonstrated lipid droplets in the cornified layers.[13] From the study of *Alox12b* mutant mouse skin transplants, it was suggested that 12R-LOX deficiency might affect the processing of LGs.[14] In *Alox12b*-disrupted mouse skin, irregular-sized vesicles were observed in the granular layers, and the stacks of lipid lamellae representing extruded content of LGs were seen in the transition zone between the uppermost granular and the first cornified cells.[11] In the present study, we clearly demonstrated lipid droplets in the cornified cell layers, and partially disturbed LG content secretion into the intercellular space in the patient's epidermis. Our results suggest that partially disturbed secretion of LG contents is involved in the pathogenesis of ichthyosis in patients with CIE with *ALOX12B* mutations. It has not been clarified completely yet how the partially disturbed secretion of LG contents contributes to the pathogenesis of CIE. Several ichthyosiform disorders have been shown to involve the abnormal function of LG.[1,15] Lipid contents secreted from LG are known to form the intercellular lipid layers in the stratum corneum.[16] The intercellular lipid layers are essential for the epidermal barrier function and the defective intercellular lipid layers caused by disturbed secretion of LG lipid contents are expected to result in skin barrier impairment.[17] Defective skin barrier function leads to compensatory mechanisms involving epidermal hyperproliferation and hyperkeratosis, which are

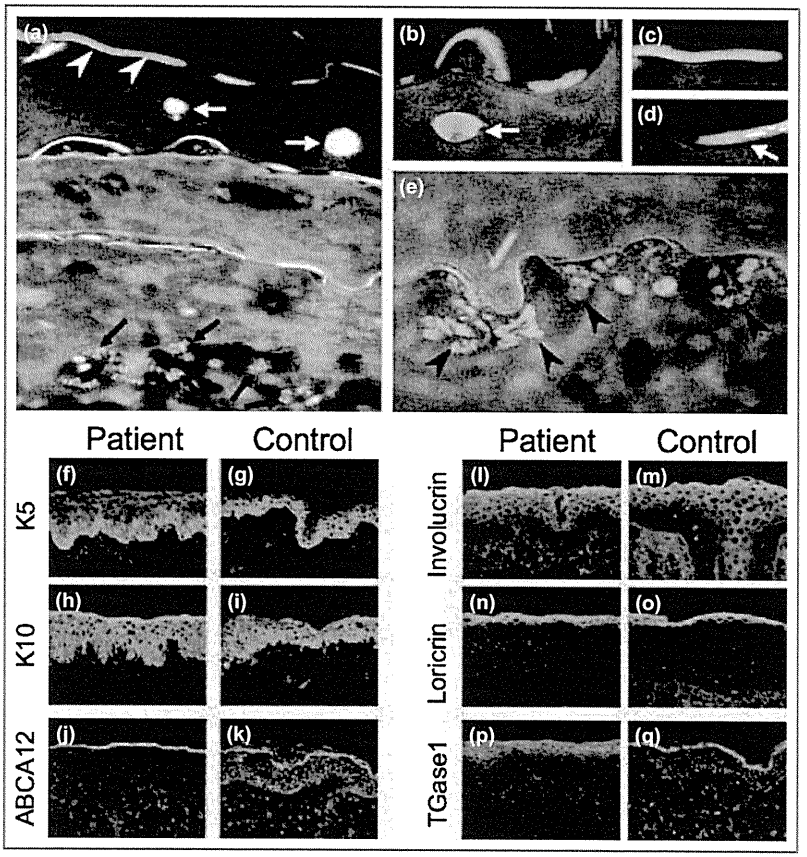

Fig 2. Disturbed secretion of lamellar granule (LG) contents from the granular layer cells and normal distribution of keratinization markers in the patient's epidermis. (a–e) Ultrastructural features of the skin biopsy specimen in the neonatal period. (a) Overall keratinization processes appeared normal. Black arrows, LGs; white arrowheads, intercellular lipid lamellae; white arrows, various-sized cytoplasmic lipid vacuoles. (b) An irregular-sized lipid vacuole (white arrow) containing the lamellar structure. (c) Intact intercellular lipid lamellae. (d) Normal cornified cell envelope (white arrow). (e) Partially congested LG secretion (arrowheads) in a granular layer cell. (f–q) Immunofluorescence staining (FITC) revealed that keratin 5, keratin 10 and ABCA12 were distributed normally in the basal layer, suprabasal layers and granular layers, respectively. For keratin 5 immunostaining, we used an antibody which cross-reacts with keratin 8. However, the labelling of this antibody is thought to reflect keratin 5 expression in this study, because keratin 8 expression is usually restricted to the simple epithelia. Cornified cell envelope-associated proteins, involucrin, loricrin and transglutaminase 1, were seen normally distributed in the upper epidermis. (f–q) Nuclear stain, red (propidium iodide). Original magnification: (a) × 6000, (b) × 12 000, (c, d) × 18 000, (e) × 10 000, (f–q) × 20.

observed frequently in ichthyosiform diseases.[16] In this context, we can hypothesize that the partially disturbed secretion of LG contents might cause defective intercellular lipid layers in the stratum corneum, resulting in skin barrier defects and subsequent compensatory hyperkeratosis in CIE.

Patients with CIE harbouring *ALOX12B* mutations have previously been reported in African and European populations.[3,4] Our previous studies failed to identify *ALOX12B* mutations in Japanese patients with ARCI[18] and demonstrated that the frequency of *ALOX12B* mutations is expected to be low in Japanese patients with ARCI. As far as we know, the present case is the first patient with CIE with detected *ALOX12B* mutations in the Asian area and our results also confirm *ALOX12B* as one of the CIE causative genes in the Asian population. Further accumulation of CIE cases is needed to clarify the frequency of *ALOX12B* mutations in patients with CIE in Asian countries.

Acknowledgments

We thank Dr James R. McMillan for proofreading this manuscript and Ms Yuki Miyamura for her fine technical assistance on this project. This work was supported in part by a Grant-in-Aid from the Ministry of Education, Science, Sports and Culture of Japan to M.A. (Kiban B 20390304) and by a grant from the Ministry of Health, Labor and Welfare of Japan (Health and Labor Sciences Research Grants; Research on Intractable Diseases; H21-047) to M.A.

References

1 Akiyama M, Shimizu H. An update on molecular aspects of the non-syndromic ichthyoses. *Exp Dermatol* 2008; **42**:83–9.

2 Jobard F, Lefèvre C, Karaduman A *et al.* Lipoxygenase-3 (*ALOXE3*) and 12(R)-lipoxygenase (*ALOX12B*) are mutated in non-bullous

congenital ichthyosiform erythroderma (NCIE) linked to chromosome 17p13.1. *Hum Mol Genet* 2002; **11**:107–13.
3 Eckl KM, de Juanes S, Kurtenbach J *et al.* Molecular analysis of 250 patients with autosomal recessive congenital ichthyosis: evidence for mutation hotspots in *ALOXE3* and allelic heterogeneity in *ALOX12B*. *J Invest Dermatol* 2009; **129**:1421–8.
4 Fischer J. Autosomal recessive congenital ichthyosis. *J Invest Dermatol* 2009; **129**:1319–21.
5 Brash AR, Yu Z, Boeglin WE, Schneider C. The hepoxilin connection in the epidermis. *FEBS J* 2007; **274**:3494–502.
6 Krieg P, Heidt M, Siebert M *et al.* Epidermis-type lipoxygenases. *Adv Exp Med Biol* 2002; **507**:165–70.
7 Anton R, Camacho M, Puig L, Vila L. Hepoxilin B3 and its enzymatically formed derivative trioxilin B3 are incorporated into phospholipids in psoriatic lesions. *J Invest Dermatol* 2002; **118**:139–46.
8 Lefèvre C, Bouadjar B, Ferrand V *et al.* Mutations in a new cytochrome P450 gene in lamellar ichthyosis type 3. *Hum Mol Genet* 2006; **15**:767–76.
9 Eckl KM, Krieg P, Küster W *et al.* Mutation spectrum and functional analysis of epidermis-type lipoxygenases in patients with autosomal recessive congenital ichthyosis. *Hum Mutat* 2005; **26**:351–61.
10 Yu Z, Schneider C, Boeglin WE, Brash AR. Mutations associated with a congenital form of ichthyosis (NCIE) inactivate the epidermal lipoxygenases 12R-LOX and eLOX3. *Biochim Biophys Acta* 2005; **3**:238–47.
11 Epp N, Fürstenberger G, Müller K *et al.* 12R-lipoxygenase deficiency disrupts epidermal barrier function. *J Cell Biol* 2007; **177**:173–82.
12 Moran J, Qiu H, Turbe-Doan A *et al.* A mouse mutation in the 12R-lipoxygenase, *Alox12b*, disrupts formation of the epidermal permeability barrier. *J Invest Dermatol* 2007; **127**:1893–7.
13 Harting M, Brunetti-Pierri N, Chan CS *et al.* Self-healing collodion membrane and mild nonbullous congenital ichthyosiform erythroderma due to 2 novel mutations in the *ALOX12B* gene. *Arch Dermatol* 2008; **144**:351–6.
14 de Juanes S, Epp N, Latzko S *et al.* Development of an ichthyosiform phenotype in *Alox12b*-deficient mouse skin transplants. *J Invest Dermatol* 2009; **129**:1429–36.
15 Hershkovitz D, Mandel H, Ishida-Yamamoto A *et al.* Defective lamellar granule secretion in arthrogryposis, renal dysfunction, and cholestasis syndrome caused by a mutation in *VPS33B*. *Arch Dermatol* 2008; **144**:334–40.
16 Elias PM. Stratum corneum defensive functions: an integrated view. *J Invest Dermatol* 2005; **125**:183–200.
17 Yanagi T, Akiyama M, Nishihara H *et al.* Harlequin ichthyosis model mouse reveals alveolar collapse and severe fetal skin barrier defects. *Hum Mol Genet* 2008; **17**:3075–83.
18 Sakai K, Akiyama M, Yanagi T *et al.* *ABCA12* is a major causative gene for non-bullous congenital ichthyosiform erythroderma. *J Invest Dermatol* 2009; **129**:2306–9.

The American Journal of Pathology, Vol. 176, No. 4, April 2010

DOI: 10.2353/ajpath.2010.090597

Short Communication

Transglutaminase1 Preferred Substrate Peptide K5 Is an Efficient Tool in Diagnosis of Lamellar Ichthyosis

Masashi Akiyama,* Kaori Sakai,* Teruki Yanagi,* Satoshi Fukushima,† Hironobu Ihn,† Kiyotaka Hitomi,‡ and Hiroshi Shimizu*

From the Department of Dermatology, Hokkaido University Graduate School of Medicine, Sapporo; the Department of Dermatology and Plastic Surgery,† Graduate School of Medical and Pharmaceutical Sciences, Kumamoto University, Kumamoto; and the Department of Applied Molecular Biosciences,‡ Graduate School of Bioagricultural Sciences, Nagoya University, Japan*

Lamellar ichthyosis (LI) is a genetically heterogeneous, severe genodermatosis showing widespread hyperkeratosis of the skin. Transglutaminase 1 (TGase1) deficiency by TGase1 gene (*TGM1*) mutations is the most prevalent cause of LI. Screening of TGase1 deficiency in skin is essential to facilitate the molecular diagnosis of LI. However, cadaverine, the most widely used substrate for TGase activity assay, is not isozyme specific. Recently, a human TGase1–specific highly preferred substrate peptide K5 (pepK5) was generated. To evaluate its potential as a diagnostic tool for LI, we performed pepK5 labeling of TGase1 activity in normal human and LI skin. Ca^{2+}-dependent labeling of FITC-pepK5 was clearly seen in the upper spinous and granular layers of normal human skin where it precisely overlapped with TGase1 immunostaining. Both specificity and sensitivity of FITC-pepK5 labeling for TGase1 activity were higher than those of FITC-cadaverine labeling. FITC-pepK5 labeling colocalized with involucrin and loricrin immunostaining at cornified cell envelope forming sites. FITC-pepK5 labeling was negative in LI patients carrying *TGM1* truncation mutations and partially abolished in the other LI patients harboring missense mutations. The present results clearly indicate that pepK5 is a powerful tool for screening LI patient TGase1 deficiency when we make molecular diagnosis of LI. *(Am J Pathol 2010, 176:1592–1599; DOI: 10.2353/ajpath.2010.090597)*

One of the essential events during terminal differentiation of epidermal keratinocytes and skin barrier formation is the production of a 15-nm-thick layer of protein on the inner surface of the keratinocyte cell membrane, termed the cornified cell envelope (CCE). The CCE is assembled by the accumulation of several precursor proteins including involucrin and loricrin.[1] It is known that the precursor proteins are cross-linked together by the formation of N^{ε}-(γ-glutamyl) lysine isodipeptide bonds catalyzed by the action of transglutaminase isoforms. Transglutaminase 1 (TGase1) is a key enzyme in CCE formation in the epidermis.

Lamellar ichthyosis (LI) is a major subtype of autosomal recessive congenital ichthyosis and clinically characterized by large, thick, dark scales over the entire body without serious background erythroderma.[2] Since the identification of TGase1 gene (*TGM1*) mutations in a number of families with LI in 1995,[3,4] more than one hundred *TGM1* mutations have been reported in LI families. TGase1 deficiency attributable to *TGM1* mutations is a major underlying causative factor in LI patients,[5,6] although LI is thought to be a genetically heterogeneous disorder and several causative molecules including TGase1 have been identified.[3,4,7,8–11] Although genotype/phenotype correlations in autosomal recessive congenital ichthyosis including LI with *TGM1* mutations have been studied for years, the exact nature of the relationship has yet to be fully elucidated.[5,6,12–15] Thus, it is difficult to know whether a causative gene is *TGM1* or not in each LI patient from each patient's clinical features alone.

Supported in part by a grant from the Ministry of Education, Science, and Culture of Japan to M.A. (Kiban B 20390304) and by a grant from Ministry of Health, Labor, and Welfare of Japan (Health and Labor Sciences Research grants; Research on intractable diseases; H21-047) to M.A.

Accepted for publication November 23, 2009.

Address reprint requests to Masashi Akiyama, M.D., Ph.D., Department of Dermatology, Hokkaido University Graduate School of Medicine, North 15 West 7, Kita-ku, Sapporo 060-8638, Japan. E-mail: akiyama@med.hokudai.ac.jp.

To date, to facilitate molecular diagnosis in LI patients with *TGM1* mutations, *in situ* transglutaminase (TGase) activity assays have been performed using cadaverine as a substrate to detect TGase1 activity in the patients' skin,[16–20] despite the fact that cadaverine is not an isozyme-specific probe, and detects total TGase activity in the epidermis. Recently, a human TGase1 specific, highly preferred substrate peptide K5 (pepK5) was generated.[21] We hypothesized that, as previously shown in mouse skin, pepK5 would detect *in situ* TGase1 activity with high specificity and sensitivity in the human epidermis. If it is the case, pepK5 can be a useful tool to detect TGase1 deficiency in LI patients with *TGM1* mutations.

In the present study, we demonstrated that pepK5 can be used as an efficient probe to detect TGase1 activity in the human epidermis. In addition, we performed *in situ* TGase1 activity assay using pepK5 in skin specimens from LI patients with *TGM1* mutations and clearly revealed that this preferred substrate for TGase1, pepK5 is a powerful tool for evaluation of TGase1 activity in LI patients and for molecular diagnosis of LI.

Materials and Methods

Synthesis of Transglutaminase Substrate Peptides

PepK5, peptide K5QN (pepK5QN), and peptide form T26 (pepT26) were synthesized as previously described.[21,22] Briefly, a phage-displayed random peptide library was used to screen primary amino acid sequences that are preferentially selected by human TGase1. The peptides selected as glutamine donor substrate exhibited a marked tendency in primary structure, conforming to the sequence: QxK/RψxxxWP (where x and ψ represent non-conserved and hydrophobic amino acids, respectively). Using glutathione S-transferase (GST) fusion proteins of the selected peptides, several sequences were identified as preferred substrates and confirmed that they were isozyme-specific. The 12-aa peptide pepK5 (YEQHKLPSSWPF) was synthesized. Even in peptide form, K5 appeared to have high and specific reactivity as substrate. In addition, a mutant peptide in which glutamine was substituted by asparagine was also synthesized as pepK5QN (YENHKLPSSWPF). pepT26 (HQSYVDPWMLDH) was synthesized as the transglutaminase 2 (TGase2) preferred substrate peptide for comparison.[22] Finally, these synthesized peptides were conjugated with FITC.[21]

In Situ *TGase1 Activity Assay*

Skin sections were prepared from skin biopsy patient specimens and normal control specimens using standard methods.[21,23] The frozen sections were dissected into 6-μm slices and stored frozen at −80°C until use.

Sections were dried and then blocked with 1% BSA in NaCl/Pi at room temperature. The sections were incubated for 90 minutes with a solution containing 100 mmol/L Tris/HCl pH 8.0, 5 mmol/L $CaCl_2$ or 1 mmol/L EDTA, and 1 mmol/L dithiothreitol, in the presence of 5 μmol/L (or other concentrations) of FITC-labeled substrate peptide or FITC-cadaverine (Sigma-Aldrich, St. Louis, MO). This *in situ* TGase1 activity assay works by measuring the fluorescence of fluorescein isothiocyanate (FITC)-labeled substrate peptide incorporated into cellular proteins by cross-linking catalyzed by TGase1. After washing with NaCl/Pi three times for 5 minutes, antifading solution was added to the sections, which were then sealed with a cover glass and mountant. In addition, we performed the above-mentioned pepK5 labeling using normal human skin specimens and LI patients' skin samples under various incubation conditions (pH 7.4, 8.0 and 8.4; temperature 25°C, 33°C and 37°C).

Double Labeling for in Situ *TGase1 Assay and Immunofluorescence Staining*

For double labeling (*in situ* TGase1 activity assay and immunofluorescence), at first, we performed *in situ* TGase1 activity assay as described above, then the sections were labeled with immunofluorescence methods below. Immunofluorescence labeling was performed as described previously.[23] Primary antibodies used in this study were as follows: mouse monoclonal anti-TGase 1 antibody (B.C1; Biomedical Technologies, Inc., Stoughton, MA), rabbit polyclonal anti-TGase1 antibody (Novus Biologicals, LLC, Littleton, CO), anti-loricrin antibody (Covance Lab., Richmond, CA), and anti-involucrin antibody (Biomedical Technologies, Inc., Stoughton, MA). We used FITC-conjugated or tetramethylrhodamine-isothiocyanate (TRITC)-conjugated rabbit anti-mouse immunoglobulin (Jackson ImmunoResearch Laboratories, Inc. West Grove, PA) or donkey anti-rabbit immunoglobulins (DAKO, Glostrup, Denmark), as secondary antibodies.

Ichthyosis Patients Involved in the Present Study

In total, four unrelated LI patients with *TGM1* mutations were included in this study. Patient 1 was a recently examined LI case and the other three patients were reported previously.[6,20,24] As controls, two *TGM1*-unrelated autosomal recessive congenital ichthyosis patients harboring ABCA12 mutations[25] were also included in the present study.

Fully informed consent was obtained from the participants or their legal guardians for this study. This study had been previously evaluated and approved by the ethics committee at Hokkaido University Graduate School of Medicine and was conducted according to the Declaration of Helsinki Principles.

Mutation Search

TGM1 mutation search was performed as previously reported.[19] Briefly, genomic DNA isolated from peripheral blood was subjected to polymerase chain reaction amplification, followed by direct automated sequencing and verification of the mutation by restriction enzyme diges-

tions. Most oligonucleotide primers used for amplification of all 15 exons of *TGM1* have been reported elsewhere[12] and partially modified for the present study.[19] The entire coding regions of *TGM1* including the exon/intron boundaries were sequenced using genomic DNA samples from patients and their family members. One hundred normal alleles (50 unrelated, healthy Japanese individuals) were sequenced as normal controls.

Results

In Situ *Assay Using pepK5 Detected TGase1 Activity with High Specificity and Sensitivity in the Upper Epidermis of Normal Human Skin*

With the presence of $CaCl_2$ in the reaction mixture, we detected specific incorporation of FITC-labeled pepK5 (FITC-pepK5; 5 μmol/L) into substrate proteins in the epidermis, mainly at the cell periphery of the upper spinous and granular layers of normal human skin (Figure 1A). No signal was detected in the presence of EDTA (Figure 1B), or when we used FITC-conjugated pepK5QN mutant peptide (FITC-pepK5QN; Figure 1C), which indicated that the cross-linking reaction was catalyzed specifically by TGase1. Using FITC-conjugated pepT26 (FITC-pepT26), a preferable substrate for TGase2, only faint labeling was obtained around the granular layer cells and this labeling was abolished in the presence of EDTA (data not shown). Under various incubation conditions, pH 7.4, 8.0, and 8.4, temperature 25°C, 33°C, and 37°C, no significant difference in the pepK5 labeling intensity was observed in normal human epidermis (data not shown).

The FITC-pepK5 labeling pattern corresponded well with the localization of TGase1 by immunostaining with anti-TGase1 antibody. Double labeling for *in situ* TGase1 activity assay using FITC-pepK5 and immunostaining for TGase1 molecule showed completely overlapping colocalization of these moieties at the cell periphery of both the upper spinous and granular layer cells (Figure 1, D–F).

Double Labeling for TGase1 Activity with pepK5 and CCE Precursor Proteins Demonstrated that pepK5 Labeling Precisely Localized to Sites of CCE Formation

Immunofluorescence labeling for involucrin, a major CCE precursor protein, was seen in the upper half of the epidermis (Figure 1H). Double labeling for *in situ* TGase1 activity assay using pepK5, and involucrin immunolabeling showed that, in the upper spinous and granular cell layers, pepK5 labeling and involucrin co-localized at the cell periphery (Figure 1, G–I). In addition, double labeling for the *in situ* TGase1 activity assay using pepK5, and immunolabeling for loricrin, another major CCE precursor protein, revealed almost complete colocalization of

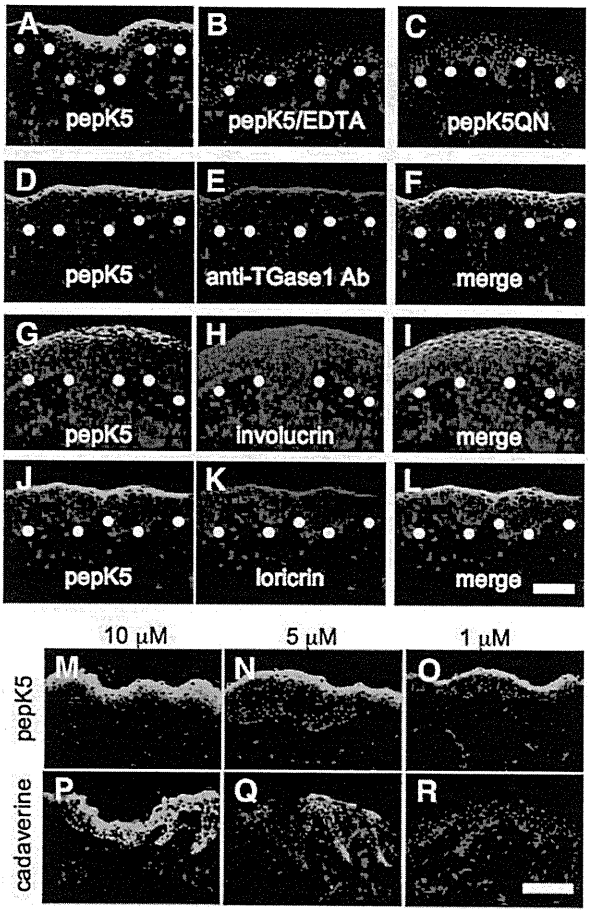

Figure 1. PepK5 labeling detected *in situ* TGase1 activity with high specificity and sensitivity at CCE forming sites in normal human skin. **A–C:** *In situ* TGase1 activity detected by pepK5 in normal skin. Detection of *in situ* TGase 1 activity using FITC-labeled pepK5 (5 μmol/L) showed intense membrane-restricted staining within the upper spinous and granular layer keratinocytes of a normal human skin (**A**). In the presence of EDTA, the pepK5 labeling was completely abolished (**B**). No labeling was observed with FITC-labeled mutant K5 peptide (pepK5QN; **C**). Specific labeling, green (FITC); nuclear stain, red (propidium iodide). **White dots**, basement membrane zone. **D–F:** Double labeling with pepK5 and anti-TGase1 antibody in normal human skin. Both pepK5 labeling (**D**, green, FITC) and anti-TGase1 antibody (B.C1) labeling (**E**, red, TRITC) are seen in the upper epidermis, mainly in the granular layers. The merged image clearly demonstrates that both labeling patterns almost completely overlap (yellow) each other on the cell membrane of the upper epidermal keratinocytes (**F**). pepK5 labeling, green (FITC), anti-TGase1 antibody labeling, red (TRITC); nuclear stain, blue (TOPRO). White dots, basement membrane zone. **G–L:** Double labeling with anti-CCE precursor protein antibodies and pepK5 in normal human skin. Anti-involucrin antibody labeling (**H**, red, TRITC) is seen in the upper half of the epidermis, although pepK5 labeling (**G**, green, FITC) is observed mainly in the uppermost spinous and granular cell layers. Involucrin and pepK5 labeling overlap each other (yellow) on the cell membrane of the uppermost spinous and granular cell layer keratinocytes in the merged image (**I**). Both pepK5 labeling (**J**, green, FITC) and anti-loricrin antibody labeling (**K**, red, TRITC) are seen mostly within the uppermost spinous and granular layers. The merged image shows that loricrin and pepK5 labeling clearly overlap (yellow) each other on the cell membrane of the granular layer keratinocytes (**L**). FITC-pepK5 labeling, green; anti-involucrin and anti-loricirn antibodies, red (TRITC); nuclear stain, blue (TOPRO). **White dots**, basement membrane zone. **M–R:** Detection of TGase1 activity in normal human skin sections using graded concentrations of pepK5 or cadaverine. Intense labeling is seen in the upper epidermis with 10 μmol/L (**M**) and 5 μmol/L (**N**) of FITC-pepK5. Only the granular layer keratinocytes are labeled with 1 μmol/L (**O**) of FITC-pepK5. Using 10 μmol/L (**P**) of FITC-cadaverine, all epidermal keratinocytes are labeled. With 5 μmol/L (**Q**) of FITC-cadaverine, entire epidermis is faintly labeled. No labeling is observed with 1 μmol/L (**R**) of FITC-cadaverine. **M–O:** FITC-pepK5 labeling, green; **P–R:** FITC-cadaverine labeling, green; nuclear stain, red (propidium iodide). Substrate concentrations, 10 μmol/L (**M**, **P**), 5 μmol/L (**N**, **Q**), 1 μmol/L (**O**, **R**). Scale bars = 50 μm.

A LI patients with *TGM1* mutations included in the present study

Patient No.	Age	Sex	*TGM1* mutations	Phenotype	Skin hyperkeratosis		References
					severity	localization	
1	0	M	p.[Arg106X]+[Gln234X]	LI (severe)	severe	generalized	this study
2	33	F	c.[371delA]+[=]	LI (severe)	severe	generalized	Ref. No. 24
3	0	M	p.[Arg307Trp]+[=]	LI (mild)	mild	localized (trunk)	Ref. No. 6
4	56	F	p.[Leu205Gln]+[Arg307Trp]	LI (mild)	mild	localized (trunk)	Ref. No. 20

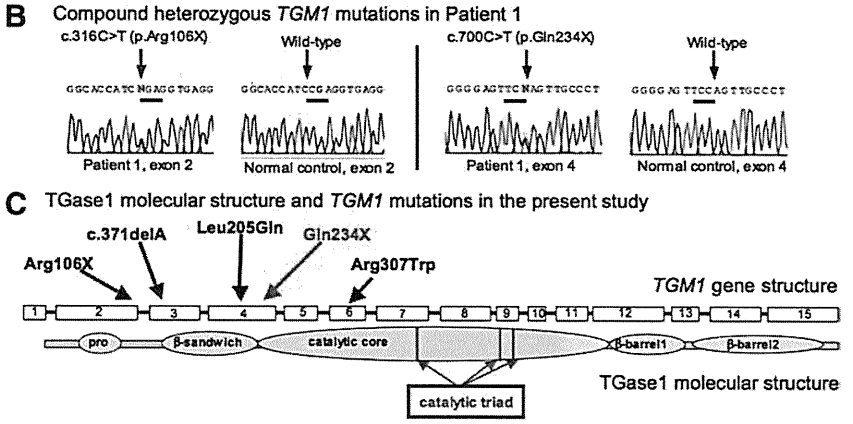

Figure 2. *TGM1* mutations and clinical features of LI patients in the present study. **A:** Summary of the *TGM1* mutations and phenotypes of the LI patients included in the present study. Note Patients 1 and 2 harbored truncation mutations in both alleles and exhibited a severe phenotype, and Patients 3 and 4 carried missense mutations in both alleles exhibiting a milder phenotype. An underlined mutation was a novel mutation. **B:** Direct sequence analysis of exons 2 and 4 of Patient 1 revealed heterozygous nonsense mutations, c.316C>T (p.Arg106X) and c.700C>T (p.Gln234X). **C:** Schematic sequential arrangement of the domain structure of the TGase1 polypeptide. Mutations in the present LI patients are marked by **arrows**. Red characters and **arrows** indicate novel mutations and black ones are previously reported mutations. Note that three truncation mutations are located upstream to the catalytic core domain. Two missense mutations are in the β-sandwich domain and the catalytic core domain, which are important for enzyme activity.

TGase1 activity and loricrin in the cell periphery of the upper spinous and granular layer cells (Figure 1, J–L).

PepK5 Detected in Situ *TGase1 Activity Efficiently Compared with Cadaverine*

We also compared the reactivity of FITC-pepK5 and FITC-cadaverine, which has been previously used for detection of *in situ* TGase activity in normal human skin at various concentrations, 10, 5, 1, and 0.1 μmol/L (Figure 1, M–R). At 10 μmol/L and 5 μmol/L concentrations, intense FITC-pepK5 labeling was observed mainly in the cell periphery of the upper spinous and granular layer keratinocytes in the normal human epidermis. At 1 μmol/L concentration, FITC-pepK5 labeled only the granular layer keratinocytes, and at 0.1 μmol/L concentration (data not shown) no FITC-pepK5 labeling was seen in the normal human epidermis. In contrast, using FITC-cadaverine at 10 μmol/L concentration, the entire epidermis was labeled, and at 5 μmol/L concentration only faint FITC-cadaverine labeling was seen in all of the layers of normal human epidermis. At 1 μmol/L or 0.1 μmol/L (data not shown) concentration, no FITC-cadaverine labeling was obtained in the epidermis. These results suggest that FITC-pepK5 detects endogenous TGase1 activity with greater sensitivity, at least more than ten times higher than FITC-cadaverine in human epidermis. In addition, considering the labeling patterns in the epidermis by the two substrates, specificity of pepK5 to TGase1 seemed to be much higher than that of cadaverine.

TGM1 Mutations and Clinical Features of LI Patients Involved in the Present Study

TGM1 mutations and clinical features of the patients included in the present study are summarized in Figure 2, A–C. Patients 1 and 2 showed a typical, classic LI phenotype. Patients 3 and 4 had a mild LI phenotype with mild hyperkeratosis mainly on the trunk. Patient 4 had a LI phenotype termed as "bathing suit ichthyosis"[26] with restricted affected regions on the trunk.

Patient 1 was a newly examined LI case. Patient 1 was compound heterozygous for the two *TGM1* nonsense mutations, p.Arg106X and p.Gln234X (c.[316C>T]+[700C>T]; p.[Arg106X]+[Gln234X]; Figure 2B) and showed a typical classic form of LI. One mutation p.Gln234X was a novel mutation and the other mutation p.Arg106X was previously reported.[27] These mutations were not found in 100 normal control alleles (50 unrelated, healthy Japanese individuals) and were not thought to be polymorphisms. The three other patients included in the present study had been reported previously to have a total of three *TGM1* mutations including p.Arg307Trp, a prevalent TGM1 mutation in the Japanese population.[6,20,24]

PepK5 Labeling Clearly Detected Defective TGase1 Activity in the Skin of LI Patients

In Patients 1 and 2, membranous TGase 1 activity detected by FITC-pepK5 in the upper spinous and granular layers of the patients' epidermis was completely lost (Figure 3, A and B). In Patient 3, membranous TGase 1 activity detected by FITC-pepK5 in the upper spinous and granular layers of the patient's epidermis was observed, but remarkably weaker (Figure 3C) than that of normal control human epidermis (Figure 3E). In Patient 4, membranous TGase1 activity demonstrated by FITC-pepK5 in the upper spinous and granular layers of the patient's epidermis was present, but restricted solely to the granular layer cells and cells just below the granular layer and was significantly weaker (Figure 3D) than that of normal control human epidermis (Figure 3E). In the

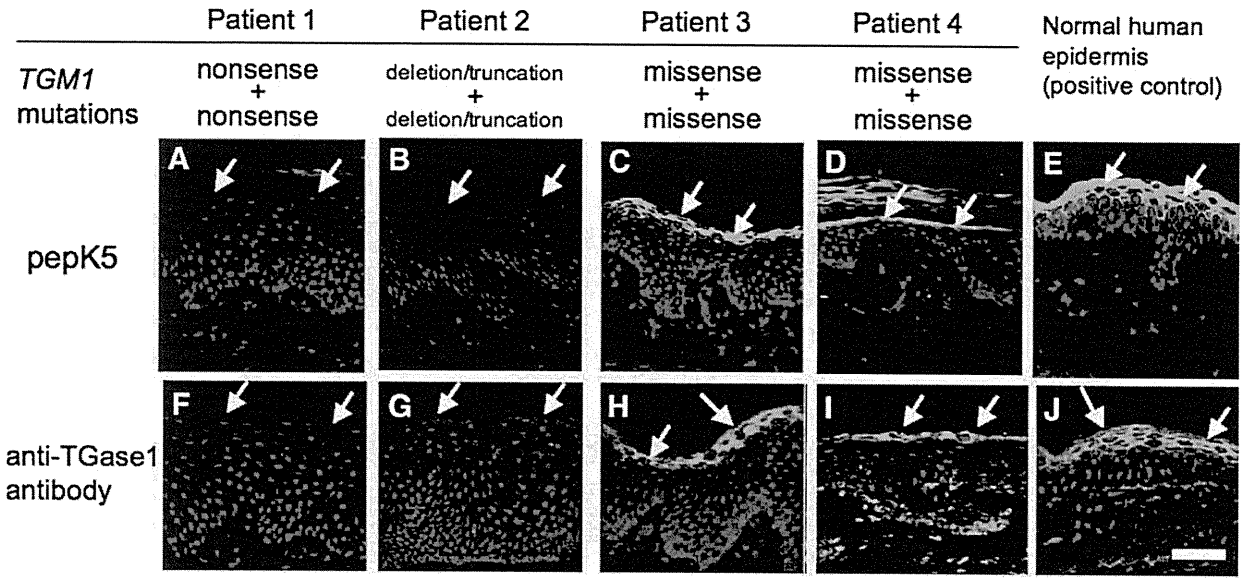

Figure 3. TGase1 deficiency detected by pepK5 labeling in the LI patients. **A and F:** Patient 1, a compound heterozygote for two *TGM1* nonsense mutations: FITC-pepK5 labeling (green) shows complete absence of TGase1 activity in the upper epidermis (**arrows**; **A**), and TGase1 immunostaining (green) is also negative in the upper epidermis (**arrows**; **F**). **B and G:** Patient 2, a homozygote for a *TGM1* deletion mutation causing truncation of the peptide: FITC-pepK5 labeling (green) reveals completely abolished TGase1 activity in the upper epidermis (**arrows**; **B**) and no TGase1 immunolabeling (in green) is seen in the upper epidermis (**arrows**; **G**). **C** and **H:** Patient 3, a homozygote for a *TGM1* missense mutation: detectable, but reduced membranous TGase1 activity is seen in the upper epidermis (**arrows**) by FITC-pepK5 labeling (green; **C**). TGase1 immunostaining (green) in the upper epidermis (**arrows**) confirms expression of TGase1 molecule (**H**). **D** and **I:** Patient 4, a compound heterozygote for two *TGM1* missense mutations: FITC-pepK5 labeling (green) shows faint TGase1 activity restricted to the granular layers (**arrows**; **D**). Immunofluorescence labeling for TGase1 (green) reveals a positive staining in the granular layer (**arrows**) in the patient's epidermis (**I**). **E and J:** In a normal human skin without any *TGM1* mutations, intense TGase1 activity is seen in the upper epidermis (**arrows**) using FITC-pepK5 labeling (green; **E**). TGase1 immunolabeling (green) is also positive in the upper epidermis (**arrows**; **J**). **A–E:** FITC-pepK5 labeling, green; **F–J:** rabbit polyclonal anti-TGase1 antibody staining, green (FITC); **A–J:** nuclear stain, red (propidium iodide). Scale bar = 50 μm.

epidermis of the two patients with ichthyosis caused by *ABCA12* mutations, other than *TGM1* mutations, intense membrane TGase1 activity was normally observed in the upper spinous and the granular layers by pepK5 labeling (data not shown).

Immunofluorescent labeling using rabbit polyclonal anti-TGase1 antibody revealed that TGase1 immunostaining was not seen in the epidermis of Patients 1 and 2 (Figure 3, F and G). In the epidermis of Patients 3 and 4, positive immunostaining for TGase1 molecule was observed mainly in the granular layer (Figure 3, H, I, and J). From the results of pepK5 labeling and immunostaining for the TGase1 molecule, in Patients 1 and 2, it was thought that immunoreactive, intact TGase1 molecule was absent from the epidermis, resulting in the absence of FITC-pepK5 labeling. In Patients 3 and 4, although immunoreactivity for TGase1 was detected in the epidermis, FITC-pepK5 labeling was remarkably weak, suggesting reduced enzyme activity of TGase1 molecules expressed in the epidermis of these patients.

In the epidermis of any LI patient, no significant difference in pepK5 labeling pattern and intensity was seen under various experimental conditions, pH 7.4, 8.0, and 8.4, temperature 25°C, 33°C, and 37°C (data not shown).

Using FITC-conjugated pepT26 (FITC-pepT26), a preferable substrate for TGase2, only faint labeling was obtained around the granular layer cells in all of the skin samples from the patients (data not shown).

Discussion

In the first half of the present study, we examined the ability of pepK5 to detect endogenous TGase1 activity in normal human skin sections. Ca^{2+}-dependent incorporation of FITC-pepK5 into glutamine acceptor substrates was clearly seen in human epidermal keratinocytes, mainly in the upper spinous and granular layers. To date, detection of cross-linked TGase products using tissue sections has used an FITC-labeled primary amine (FITC-cadaverine) or FITC-labeled substrate peptides.[28,29] The pattern of TGase activity that we observed was consistent with that seen in the skin using FITC-cadaverine.[29] In addition, the staining sensitivity of pepK5 was remarkably higher than that of cadaverine in normal human epidermis.

As observed in immunostaining analysis, TGase1 protein localizes to the peripheral regions of the keratinocytes in the granular and upper spinous layers, consistent with previous reports.[30,31] Double fluorescence staining clearly indicated that TGase1 activity labeled with pepK5 precisely colocalized with TGase1 immunolabeling at these sites. In addition, TGase1 activity demonstrated with pepK5 overlapped with the major CCE precursor proteins, loricrin and involucrin. These findings confirm that pepK5 labeling specifically demonstrates TGase1 activity at sites of CCE formation. In the *in vitro* assay with TGase2, pepK5 reacted to a small extent at high peptide concentration.[21] Thus, in the present study,

it was necessary to check endogenous TGase2 activity in the skin samples and we confirmed that there was no significant TGase2 activity in the skin sections by FITC-labeled pepT26 labeling. From these results, we conclude that pepK5 can act as a highly sensitive and specific probe to detect *in situ* endogenous TGase1 activity in the human epidermis.

In the last half of the present study, to assess the efficacy and usefulness of pepK5 as a preferred substrate for TGase1 in evaluating TGase1 activity in LI patients, we performed *in situ* TGase1 activity assays using pepK5 as a substrate in four LI patients with *TGM1* mutations.

From the nature and sites of *TGM1* mutations in each patient and their effect on TGase1 activity, according to the protein modeling of TGase1 based on the structure of the human factor XIIIa subunit,[32] a level of remnant TGase1 activity was theoretically speculated in each case as follows.

Patient 1 is a compound heterozygote for *TGM1* nonsense mutations (Figure 2). Both nonsense mutations led to truncation of the catalytic core domain and are expected to result in a complete loss of function of TGase1 activity. Patient 2 is a homozygote for a *TGM1* deletion mutation resulting in a frameshift and premature termination in an upstream of the catalytic core domain (Figure 2). Thus, TGase1 activity is also expected to be completely abolished in the epidermis of Patient 2. In addition, all of the three truncation mutations in Patients 1 and 2 led to early termination codons. This would probably lead to complete lack of the polypeptide in the present Patients 1 and 2. Furthermore, genomic premature termination codon mutations are subject to nonsense-mediated mRNA decay resulting in mRNA degradation in some instances, depending on the mutation site.[33,34]

Patient 3 is a homozygote of a missense mutation in the center of catalytic core domain of TGase1 peptide (Figure 2). Homozygosity of this mutation is expected to result in a significant, but not complete loss of TGase1 function. Patient 4 is a compound heterozygote harboring a missense mutation in the β-sandwich domain, and the missense mutation in the center of catalytic core domain, identical to the mutation harbored by Patient 3 (Figure 2). As described above, the latter mutation in the catalytic core domain is expected to lead to a significant but only partial loss of activity of TGase1. The former mutation p.Leu204Gln in the β-sandwich domain is considered to alter protein folding, which in turn affects the protein stability of TGase 1, as suggested in other missense mutations in the β-sandwich domain.[12] This instability may result in rapid degradation of the TGase1 polypeptide and reduce TGase1 activity in the patient's epidermis, although the reduction in activity might not be as serious compared with truncation mutations in Patients 1 and 2. In addition to this simplistic view based on the position of missense mutations in the primary structure, it has been demonstrated that *TGM1* mutations in specific residues have their specific effects on the TGase1 activity, leading to specific phenotypes. For example, the distinct phenotype of self-healing collodion baby can be caused by compound heterozygous *TGM1* mutations p.Gly278Arg and p.Asp490Gly.[35] Molecular modeling and biochemical assays suggested that the high hydrostatic pressure *in utero* significantly inhibit the mutant TGase1 activity. After birth, the mutant TGase1 molecules become partially active under ordinary hydrostatic pressure, resulting in the dramatic improvement of skin symptoms in a self-healing collodion baby.[35] In addition, several *TGM1* missense mutations in specific residues were reported to cause another specific phenotype, bathing suit ichthyosis, characterized by pronounced scaling restricted to the bathing suit areas.[26,36] The affected sites are warmer body areas, and bathing suit ichthyosis is thought to be a temperature-sensitive phenotype.[26] A marked decrease of *in situ* TGase1 activity was revealed at high temperature (37°C) in the patients with bathing suit ichthyosis.[26] Recent findings have shown that wild-type TGase1 activity is clearly reduced at 25°C compared with 37°C by *in vivo* activity analysis with cadaverine as a substrate. On the other hand, in case of reconstituted mutant TGase1 molecules with the specific mutations in bathing suit ichthyosis, such as p.Arg307Gly, the TGase1 activity is increased at 33°C (and even higher at 31°C) compared with 37°C.[37] In the present study, under various temperature incubation conditions, 25°C, 33°C, and 37°C, no significant difference in the pepK5 labeling intensity was observed in normal human epidermis or in the epidermis of any LI patient, although Patient 4 had a missense mutation in Arg307 (p.Arg307Trp) in which another mutation p.Arg307Gly causing bathing suit ichthyosis phenotype was previously reported.[26] We think these discrepancies on temperature sensitivity between previous reports[26,37] and our present results may be attributable to the fact that fluorescence labeling is not completely a quantitative method. In addition, we incubated tissue sections with a substrate solution for 90 minutes in our *in situ* TGase1 activity assay. Thus, we cannot exclude the possibility that the long-time incubation might make the enzymatic reaction almost saturated and make it difficult to detect fine difference in TGase1 activity.

As the results of the present study, *in situ* TGase1 activity assays using pepK5 demonstrated a remarkably reduced or a complete lack of membrane-associated labeling in the epidermis in all patients with *TGM1* mutations compared with normal human epidermis and ichthyosis patients with *TGM1*-unrelated genetic defects. The present results indicate that pepK5 labeling can distinguish LI patients with *TGM1* mutations from normal healthy individuals and from ichthyosis patients with other causative gene mutations. In this context, specific and sensitive detection of TGase1 activity using pepK5 is thought to be a powerful tool for screening TGase1 deficiency in LI patients. Furthermore, in the present LI patients, we demonstrated that the TGase1 molecule was missing in a compound heterozygote and a homozygote for *TGM1* nonsense/truncation mutations and was present in a compound heterozygote and a homozygote for missense mutations. Accordingly, pepK5 labeling was missing in the patients with nonsense/truncation mutations, although there were weaker pepK5 signals in the patients with missense mutations. In this context, it might

be possible to differentiate LI patients with nonsense/truncation mutations and those with missense mutations, and to predict patients' clinical severity and courses from pepK5 labeling results. However, pepK5 fluorescence labeling is not a completely quantitative method and further accumulation of the pepK5 labeling data in LI cases with *TGM1* mutations is needed for its diagnostic application, especially for the prediction of clinical severity in patients.

Acknowledgments

We thank Akari Nagasaki, M.S. for her technical assistance and Associate Professor James R. McMillan for proofreading this manuscript.

References

1. Steinert PM, Marekov LN: The proteins elafin, filaggrin, keratin intermediate filaments, loricrin, and small proline-rich proteins 1 and 2 are isodipeptide cross-linked components of the human epidermal cornified cell envelope. J Biol Chem 1995, 70:17702–17711
2. Akiyama M: Harlequin ichthyosis and other autosomal recessive congenital ichthyoses: the underlying genetic defects and pathomechanisms. J Dermatol Sci 2006, 42:83–89
3. Huber M, Rettler I, Bernasconi K, Frenk E, Lavrijsen SP, Ponec M, Bon A, Lautenschlager S, Schorderet DF, Hohl D: Mutations of keratinocyte transglutaminase in lamellar ichthyosis. Science 1995, 267:525–528
4. Russell LJ, DiGiovanna JJ, Rogers GR, Steinert PM, Hashem N, Compton JG, Bale SJ: Mutations in the gene for transglutaminase 1 in autosomal recessive lamellar ichthyosis. Nat Genet 1995, 9:279–283
5. Herman ML, Farasat S, Steinbach PJ, Wei MH, Toure O, Fleckman P, Blake P, Bale SJ, Toro JR: Transglutaminase-1 gene mutations in autosomal recessive congenital ichthyosis: summary of mutations (including 23 novel) and modeling of TGase-1. Hum Mutat 2009, 30:537–547
6. Sakai K, Akiyama M, Yanagi T, McMillan JR, Suzuki T, Tsukamoto K, Sugiyama H, Hatano Y, Hayashitani M, Takamori K, Nakashima Keiko, Shimizu H: ABCA12 is a major causative gene for non-bullous congenital ichthyosiform erythroderma. J Invest Dermatol 2009, 129:2306–2309
7. Akiyama M, Shimizu H: An update on molecular aspects of the non-syndromic ichthyoses. Exp Dermatol 2008, 17:373–382
8. Jobard F, Lefévre C, Karaduman A, Blanchet-Bardon C, Emre S, Weissenbach J, Ozgüc M, Lathrop M, Prud'homme JF, Fischer J: Lipoxygenase-3 (ALOXE3) and 12(R)-lipoxygenase (ALOX12B) are mutated in non-bullous congenital ichthyosiform erythroderma (NCIE) linked to chromosome 17p13.1. Hum Mol Genet 2002, 1:107–113
9. Lefévre C, Audebert S, Jobard F, Bouadjar B, Lakhdar H, Boughdene-Stambouli O, Blanchet-Bardon C, Heilig R, Foglio M, Weissenbach J, Lathrop M, Prud'homme JF, Fischer J: Mutations in the transporter ABCA12 are associated with lamellar ichthyosis type 2. Hum Mol Genet 2003, 12:2369–2378
10. Lefévre C, Bouadjar B, Karaduman A, Jobard F, Saker S, Ozgüc M, Lathrop M, Prud'homme JF, Fischer J: Mutations in ichthyin a new gene on chromosome 5q33 in a new form of autosomal recessive congenital ichthyosis. Hum Mol Genet 2004, 13:2473–2482
11. Lefévre C, Bouadjar B, Ferrand V, Tadini G, Mégarbané A, Lathrop M, Prud'homme JF, Fischer J: Mutations in a new cytochrome P450 gene in lamellar ichthyosis type 3. Hum Mol Genet 2006, 15:767–776
12. Laiho E, Ignatius J, Mikkola H, Yee VC, Teller DC, Niemi KM, Saarialho-Kere U, Kere J, Palotie A: Transglutaminase 1 mutations in autosomal recessive congenital ichthyosis: private and recurrent mutations in an isolated population. Am J Hum Genet 1997, 61:529–538
13. Hennies HC, Küster W, Wiebe V, Krebsová A, Reis A: Genotype/phenotype correlation in autosomal recessive lamellar ichthyosis. Am J Hum Genet 1998, 62:1052–1061
14. Laiho E, Niemi K-M, Ignatius J, Kere J, Palotie A, Saarialho-Kere U: Clinical and morphological correlations for transglutaminase 1 gene mutations in autosomal recessive congenital ichthyosis. Eur J Hum Genet 1999, 7:625–632
15. Shevchenko YO, Compton JG, Toro JR, DiGiovanna JJ, Bale SJ: Splice-site mutation in TGM1 in congenital recessive ichthyosis in American families: molecular, genetic, genealogic, and clinical studies. Hum Genet 2000, 106:492–499
16. Aeschlimann D, Wetterwald A, Fleisch H, Paulsson M: Expression of tissue transglutaminase in skeletal tissues correlates with events of terminal differentiation of chondrocytes. J Cell Biol 1993, 120:1461–1470
17. Raghunath M, Hennies HC, Velten F, Wiebe V, Steinert PM, Reis A, Traupe H: A novel in situ method for the detection of deficient transglutaminase activity in the skin. Arch Dermatol Res 1998, 290:621–627
18. Hohl D, Aeschlimann D, Huber M: In vitro and rapid in situ transglutaminase assays for congenital ichthyoses—a comparative study. J Invest Dermatol 1998, 110:268–271
19. Akiyama M, Takizawa Y, Kokaji T, Shimizu H: Novel mutations of TGM1 in a child with congenital ichthyosiform erythroderma. Br J Dermatol 2001, 144:401–407
20. Akiyama M, Takizawa Y, Suzuki Y, Ishiko A, Matsuo I, Shimizu H: Compound heterozygous TGM1 mutations including a novel missense mutation L204Q in a mild form of lamellar ichthyosis. J Invest Dermatol 2001, 116:992–995
21. Sugimura Y, Hosono M, Kitamura M, Tsuda T, Yamanishi K, Maki M, Hitomi K: Identification of preferred substrate sequences for transglutaminase 1 – development of a novel peptide that can efficiently detect cross-linking enzyme activity in the skin. FEBS J 2008, 275:5667–5677
22. Sugimura Y, Hosono M, Wada F, Yoshimura T, Maki M, Hitomi K: Screening for the preferred substrate sequence of transglutaminase using a phage-displayed peptide library. Identification of peptide substrates for TGase2 and factor XIIIa J Biol Chem 2006, 281:17699–17706
23. Akiyama M, Smith LT, Shimizu H: Expression of transglutaminase activity in developing human epidermis. Br J Dermatol 2000, 142:223–225
24. Akiyama M, Takizawa Y, Suzuki Y, Shimizu H: A novel homozygous mutation 371delA in TGM1 leads to a classic lamellar ichthyosis phenotype. Br J Dermatol 2003, 148:149–153
25. Natsuga K, Akiyama M, Kato N, Sakai K, Sugiyama-Nakagiri Y, Nishimura M, Hata H, Abe M, Arita K, Tsuji-Abe Y, Onozuka T, Aoyagi S, Kodama K, Ujiie H, Tomita Y, Shimizu H: Novel ABCA12 mutations identified in two cases of non-bullous congenital ichthyosiform erythroderma associated with multiple skin malignant neoplasia. J Invest Dermatol 2007, 127:2669–2673
26. Oji V, Hautier JM, Ahvazi B, Hausser I, Aufenvenne K, Walker T, Seller N, Steijlen PM, Küster W, Hovnanian A, Hennies HC, Traupe H: Bathing suit ichthyosis is caused by transglutaminase-1 deficiency: evidence for a temperature-sensitive phenotype. Hum Mol Genet 2006, 15:3082–3097
27. Esposito G, Tadini G, Paparo F, Viola A, Ieno L, Pennacchia W, Messina F, Giordano L, Piccirillo A, Auricchio L: Transglutaminase 1 deficiency and corneocyte collapse: an indication for targeted molecular screening in autosomal recessive congenital ichthyosis. Br J Dermatol 2007, 157:808–810
28. Furutani Y, Kato A, Notoya M, Ghoneim MA, Hirose S: A simple assay and histochemical localization of transglutaminase activity using a derivative of green fluorescent protein as substrate. J Histochem Cytochem 2001, 49:247–258
29. Oji V, Oji ME, Adamini N, Walker T, Aufenvenne K, Raghunath M, Traupe H: Plasminogen activator inhibitor-2 is expressed in different types of congenital ichthyosis: in vivo evidence for its cross-linking into the cornified cell envelope by transglutaminase-1. Br J Dermatol 2006, 154:860–867
30. Hiiragi T, Sasaki H, Nagafuchi A, Sabe H, Shen SC, Matsuki M, Yamanishi K, Tsukita S: Transglutaminase type 1 and its cross-linking activity are concentrated at adherens junctions in simple epithelial cells. J Biol Chem 1999, 274:34148–34154
31. Iizuka R, Chiba K, Ohmi-Imajoh S: A novel approach for the detection of proteolytically activated transglutaminase 1 in epidermis using cleavage site-directed antibodies. J Invest Dermatol 2003, 121:457–464
32. Yee VC, Pedersen LC, Le Trong I, Bishop PD, Stenkamp RE, Teller DC: Three-dimensional structure of a transglutaminase: human blood coagulation factor XIII. Proc Natl Acad Sci USA 1994, 91:7296–7300
33. Maquat LE: Nonsense-mediated mRNA decay: splicing, translation and mRNP dynamics. Nat Rev Mol Cell Biol 2004, 5:89–99

34. Lejeune F, Maquat LE: Mechanistic links between nonsense-mediated mRNA decay and pre-mRNA splicing in mammalian cells. Curr Opin Cell Biol 2005, 17:309–315
35. Raghunath M, Hennies HC, Ahvazi B, Vogel M, Reis A, Steinert PM, Traupe H: Self-healing collodion baby: a dynamic phenotype explained by a particular transglutaminase-1 mutation. J Invest Dermatol 2003, 120:224–228
36. Arita K, Jacyk WK, Wessagowit V, van Rensburg EJ, Chaplin T, Mein CA, Akiyama M, Shimizu H, Happle R, McGrath JA: The South African "bathing suit ichthyosis" is a form of lamellar ichthyosis caused by a homozygous missense mutation, p.R315L, in transglutaminase 1. J Invest Dermatol 2007, 127:490–493
37. Aufenvenne K, Oji V, Walker T, Becker-Pauly C, Hennies HC, Stöcker W, Traupe H: Transglutaminase-1 and bathing suit ichthyosis: molecular analysis of gene/environment interactions. J Invest Dermatol 2009, 129:2068–2071

Journal of Dermatological Science 57 (2010) 183–191

Contents lists available at ScienceDirect

Journal of Dermatological Science

journal homepage: www.elsevier.com/jds

Topical application of anti-angiogenic peptides based on pigment epithelium-derived factor can improve psoriasis

Riichiro Abe [a,1,*], Sho-ichi Yamagishi [b,1], Yasuyuki Fujita [a], Daichi Hoshina [a], Mikako Sasaki [a], Kazuo Nakamura [b], Takanori Matsui [b], Tadamichi Shimizu [c], Richard Bucala [d], Hiroshi Shimizu [a]

[a] Department of Dermatology, Hokkaido University Graduate School of Medicine, Sapporo, Japan
[b] Department of Pathophysiology and Therapeutics of Diabetic Vascular Complications, Kurume University School of Medicine, Kurume, Japan
[c] Department of Dermatology, Toyama University School of Medicine, Toyama, Japan
[d] Department of Internal Medicine, Yale University School of Medicine, New Haven, CT, USA

ARTICLE INFO

Article history:
Received 5 August 2009
Received in revised form 17 December 2009
Accepted 17 December 2009

Keywords:
Angiogenesis
Keratinocyte
Psoriasis
Pigment epithelium-derived factor
Vascular endothelial growth factor

ABSTRACT

Background: Psoriasis is a common chronic inflammatory skin disorder with a high prevalence (3–5%) in the Caucasian population. Although the number of capillary vessels increases in psoriatic lesions, there have been few reports that have specifically examined the role of angiogenesis in psoriasis. Angiogenic factors, such as vascular endothelial growth factor (VEGF), may dominate the activity of anti-angiogenic factors and accelerate angiogenesis in psoriatic skin.
Objective: We investigated to identify small peptide mimetics of PEDF that might show anti-angiogenic potential for the topical treatment for psoriasis.
Methods: We examined the expression of PEDF in skin by immunohistochemical staining, immunoblotting, and RT-PCR. To identify potential PEDF peptides, we screened peptides derived from the proteolytic fragmentation of PEDF for their anti-proliferative action. Anti-psoriatic functions of these peptides were analyzed using a mouse graft model of psoriasis.
Results: The specific low-molecular weight peptides (MW < 850 Da) penetrated the skin and showed significant anti-angiogenic activity in vitro. Topical application of these peptides in a severe combined immunodeficient mouse model of psoriatic disease led to reduced angiogenesis and epidermal thickness.
Conclusions: These data suggest that low-molecular PEDF peptides with anti-angiogenic activity may be a novel therapeutic strategy for psoriasis.

1. Introduction

Psoriasis is a common skin disease affecting 0.5–3% of the Caucasian population [1]. Histopathologically, this disorder is characterized by accelerated epidermal proliferation, by the infiltration of inflammatory cells into the epidermis and upper dermis, and by telangiectasia in the superficial dermis. Although the molecular pathogenesis of psoriasis remains unclear, several hypotheses have been proposed. Activated T lymphocytes infiltrate into the lesional skin areas where they secrete a variety of cytokines such as tumor necrosis factor (TNF)-α, interferon-γ, IL-2 and IL-12, and thus play an important role in psoriatic inflammatory changes [2]. In addition, epidermal proliferation is influenced by inappropriate vascular expansion in the superficial dermis [3]. Furthermore, these microvascular changes in psoriatic skin lesions include pronounced capillary dilatation, increased vessel permeability and endothelial cell proliferation and protrusion into the dermal papillae capillaries. Therefore inappropriate angiogenic growth has been proposed to contribute to the pathogenesis of psoriasis [4,5]. The overexpression of angiogenic factors also occurs; for instance, vascular endothelial growth factor (VEGF) is strongly up-regulated in psoriatic skin lesions [6].

There have been a number of therapeutic strategies devised for psoriasis. Topical steroids, topical vitamin D3 analogs, oral retinoids, UV irradiation such as PUVA and narrow-band UVB, cyclosporine and other immunosuppressants have been widely used. In addition, biological agents that target cytokines such as TNF-α have recently been developed [7]. Most strategies are aimed at reducing the inflammatory reaction and epidermal proliferation, but yet there have been few agents targeting angiogenesis in psoriasis.

Pigment epithelium-derived factor (PEDF) is a glycoprotein that belongs to the superfamily of serine protease inhibitors, and it was

Abbreviations: PEDF, pigmented epithelium-derived factor; VEGF, vascular endothelial growth factor.

* Corresponding author at: Department of Dermatology, Hokkaido University Graduate School of Medicine, N 15 W 7, Kita-ku, Sapporo 060-8638, Japan. Tel.: +81 11 706 7387; fax: +81 11 706 7820.
E-mail address: aberi@med.hokudai.ac.jp (R. Abe).
[1] These authors contributed equally to this paper.

0923-1811/$36.00
doi:10.1016/j.jdermsci.2009.12.010

first identified as a retinal pigment epithelium-derived protein with neuronal differentiating activity [8]. Recently, PEDF has been shown to have potent anti-angiogenic activity in cell culture and in animal models. PEDF inhibits retinal endothelial cell growth and migration, and it suppresses ischemia-induced retinal neovascularization [9]. In addition, we reported that PEDF inhibits malignant melanoma growth by suppressing tumor angiogenesis [10]. These observations led us to hypothesize that an imbalance in anti-angiogenic factors potentially involving PEDF may contribute to the pathogenesis of psoriasis. PEDF also shows anti-inflammatory activity, suggesting an additional, ameliorative role in the control of inflammation and keratinocyte proliferation.

In this study, we examined PEDF protein production in psoriasis lesions and in normal skin, and we investigated the effect of PEDF on keratinocyte proliferation in vitro and on psoriatic skin in a murine xenograft model. We also report the identification of low molecular weight PEDF peptides that show anti-angiogenic activity after topical application.

2. Experimental procedures

2.1. Patients

Sera were obtained from 21 psoriasis patients (13 males and 8 females, and mean age 46.9 years) and 14 healthy volunteers (males 7 and females 7, and mean age 42.2 years) from the Department of Dermatology, Hokkaido University Hospital. The diagnosis of psoriasis was made on the basis of clinical images and histopathological findings from skin biopsies. The enrolled patients had generalized plaque psoriasis, which were evaluated by a single qualified dermatologist. Three skin tissue specimens were obtained from each psoriatic lesion. Normal skin tissues also were obtained from healthy volunteers. Informed consent was obtained from each volunteer according to the Declaration of Helsinki Principles. All the experiments using human samples were performed under the approval of the ethical committee of Hokkaido University.

2.2. Experimental mice

The C.B-17/Icr-scid/scidJcl SCID mouse (Clea, Tokyo, Japan) was used for xenotransplantation experiments. All the animal experiments were performed under the approval of the ethical committee for animal studies in Hokkaido University.

2.3. Immunohistochemistry

The paraffin-embedded skin tissues from psoriasis patients were cut into 4 μm-thick sections. The sections were deparaffinized, incubated with 0.1% trypsin at 37 °C for 15 min. Endogenous peroxidase activity was inhibited by pretreatment with 3% hydrogen peroxide. The sections were then treated with 10% normal goat serum at room temperature for 30 min, followed by incubation with the anti-PEDF antibody (Santa Cruz Biotechnology, Santa Cruz, CA) at 4 °C overnight. After washing, the sections were incubated with horseradish peroxidase (HRP)-conjugated goat anti-rabbit IgG at room temperature for 30 min and the PEDF-positive staining visualized with diaminobenzidine (Dojin, Kumamoto, Japan) as a chromogen and hematoxylin as a counterstain.

For immunofluorescence, skin tissues were immediately embedded in optimal cutting temperature (OCT) reagent (Sakura Finetechnical, Tokyo, Japan) and snap-frozen in liquid nitrogen. Cryosections of 5 μm were prepared, washed with PBS, and then fixed in cold acetone for 10 min at −20 °C. Primary and secondary antibodies were applied at room temperature for 1 h. The sections were finally washed with PBS and mounted on microscope slides. The samples were analyzed using a Fluoview confocal laser scanning microscope (Olympus, Nagano, Japan). The following antibodies were used: rat anti-mouse CD31 antibody, anti-mouse CD3 antibody, anti-mouse Gr-1 antibody, and anti-mouse CD11b antibody (BD Biosciences, San Jose, CA), rabbit polyclonal anti-pankeratin antibody (PROGEN Biotechnik, Heidelberg, Germany), rabbit polyclonal anti-Ki67 antibody (Novocastra, Newcastle, UK), FITC-conjugated goat anti-rabbit antibody, FITC-conjugated goat anti-rat antibody (Jackson ImmunoResearch, West Grove, PA), TRITC-conjugated anti-rabbit antibody (Southern Biotechnology Associates, Birmingham, AL).

2.4. Immunoblots

Skin tissues of normal volunteers and psoriasis patients were treated with 1 M sodium hydroxide at 4 °C overnight, and the epidermal sheets easily removed from the dermal components. These tissues were frozen and then homogenized in PBS. Samples obtained from epidermis and dermis were electrophoresed on SDS–PAGE. Proteins on the gel were electrophoretically transferred to a nitrocellulose membrane (Bio-Rad, Hercules, CA) and the membranes probed with first antibody at 4 °C overnight, washed three times for 5 min, and then incubated with HRP-conjugated secondary antibodies at room temperature for 1 h. Proteins were visualized with a Konica immunostaining kit (Konica, Tokyo, Japan). The following antibodies were used: anti-PEDF and anti-VEGF rabbit polyclonal antibody (Santa Cruz Biotechnology), anti-α-tubulin mouse monoclonal antibody (Sigma, St. Louis, MO), HRP-conjugated goat anti-rabbit IgG, and HRP-conjugated goat anti-mouse IgG (Biosource, Camarillo, CA). We used anti-PEDF at 1:200, and the secondary antibodies at 1:1000 dilutions.

2.5. RT-PCR analysis

RNA (0.5 μg) was used to produce cDNA using a reverse transcription kit (Sigma, Poole, Dorset, United Kingdom). PCR was done using a 2400 thermocycler (Perkin-Elmer, Norwalk CT) with conditions set to 40 s at 94 °C, 60 s at 55 °C, and 60 s at 72 °C (30 cycles). The quality of DNA was verified by 0.59 kb β-actin PCR products using primers (forward 5′-ATGATATCGCCGCGCTCGTC-3′; reverse 5′-CGCTCGGTGAGGATCTTCA-3′). PEDF forward and reverse primers were 5′-GGTGCTACTCCTCTGCATT-3′ and 5′-ACTGAACCTGACCGTACAAGAAAGGATCCTCCTCCTC-3′. PCR products were separated by 2% agarose gel and visualized under UV light following ethidium bromide staining.

2.6. Preparations of PEDF proteins

The PEDF proteins were purified as described previously [9]. Briefly, 293T cells (ATCC, Rockville, MD, USA) were transfected with the recombinant vector pBK-CMV-C terminally hexahistidine-tagged PEDF using FuGENE® 6 transfection reagent (Roche Diagnostics, Mannheim, Germany) according to the manufacturer's instructions. The PEDF proteins were purified from conditioned media by a Ni-NTA spin kit (Qiagen, Hilden, Germany) according to the manufacturer's recommendation. Sodium dodecyl sulphate–polyacrylamide gel electrophoresis (SDS–PAGE) of purified PEDF proteins revealed a single band with a molecular mass of about 50 kDa, which showed positive reactivity with monoclonal antibodies directed against human PEDF (Transgenic, Kumamoto, Japan).

2.7. PEDF enzyme-linked immunosorbent assay

A PEDF enzyme-linked immunosorbent assay was performed as previously reported [11]. Briefly, a 96-well microtiter plate (Nalge

Nunc International, Rochester, NY) was coated by overnight incubation with anti-PEDF monoclonal antibody (Transgenic, Kumamoto, Japan). Samples were diluted 50-fold in 10 mM PBS pH 7.4, 0.25% BSA and 0.05% Tween-20, and then incubated at room temperature for 2 h. After washing, a biotinylated anti-human PEDF polyclonal antibody (R&D Systems, Minneapolis, MN) was added and incubation continued for 2 h at room temperature. The plate was then incubated with HRP-conjugated streptavidine solution (Zymed, South San Francisco, CA) at room temperature for 30 min. After washing, the chromogenic substrate solution (Dako, Tokyo, Japan) was added and the plate was incubated at room temperature for 15 min. Optical densities were measured at 450 nm and protein concentrations calculated from a standard curve generated by a curve-fitting program (Berthold Technology, Bad Wildbad, Germany).

2.8. PEDF secretion from cultured keratinocytes and fibroblasts

Normal human epidermal keratinocytes (NHEKs) were purchased from Clontech (Mountain View, CA and cultured in KGM® medium (Cambrex, East Rutherford, NJ) until 70% confluence. Normal human fibroblasts were purchased from Dainippon Seiyaku (Osaka, Japan) and cultured in Dulbecco's Modified Eagle's Medium (DMEM) (Invitrogen, Carlsbad, CA) containing 10% FBS, 1% penicillin, 1% streptomycin and 1% amphotericin B until 70% confluence. The cells were expanded in 12 cm sterile culture dish with 10 ml of medium, and then stimulated with lipopolysaccharide (Sigma) at 37 °C for 72 h. Media was collected 1 day after stimulation. PEDF concentrations in collected medium were assessed by ELISA as described above.

2.9. Keratinocyte proliferation assay

NHEKs were seeded into 96-well plates at a concentration of 10^3 cells in 100 μl of medium per well. After cultivation with 1, 10, 100 nM recombinant PEDF [12] and/or 100 ng/ml recombinant VEGF (R&D systems) for 2 and 4 days, 10 μl of Cell Counting Kit (Dojin) was added to each well. After incubation for 2 h, the absorbance at 450 nm was measured on a microplate reader.

2.10. Treatment of the grafted skin lesions with recombinant PEDF

A graft bed of approximately 1 cm^2 was created on the shaved area of the back of a 7 to 8-week-old anesthetized SCID mouse by removing the full-thickness skin and keeping the vessel plexus intact on the fascia overlying back muscles. The human skin obtained by biopsy was washed in PBS containing 1% penicillin, 1% streptomycin and 1% amphotericin B, and fatty deposits were removed by gentle dissection. The full-thickness human skin graft was placed onto wound bed. The transplants were held in place using 5/0 silk suture material, and 1% gentamicin sulfate ointment was applied. The graft was covered with an adhesive wound

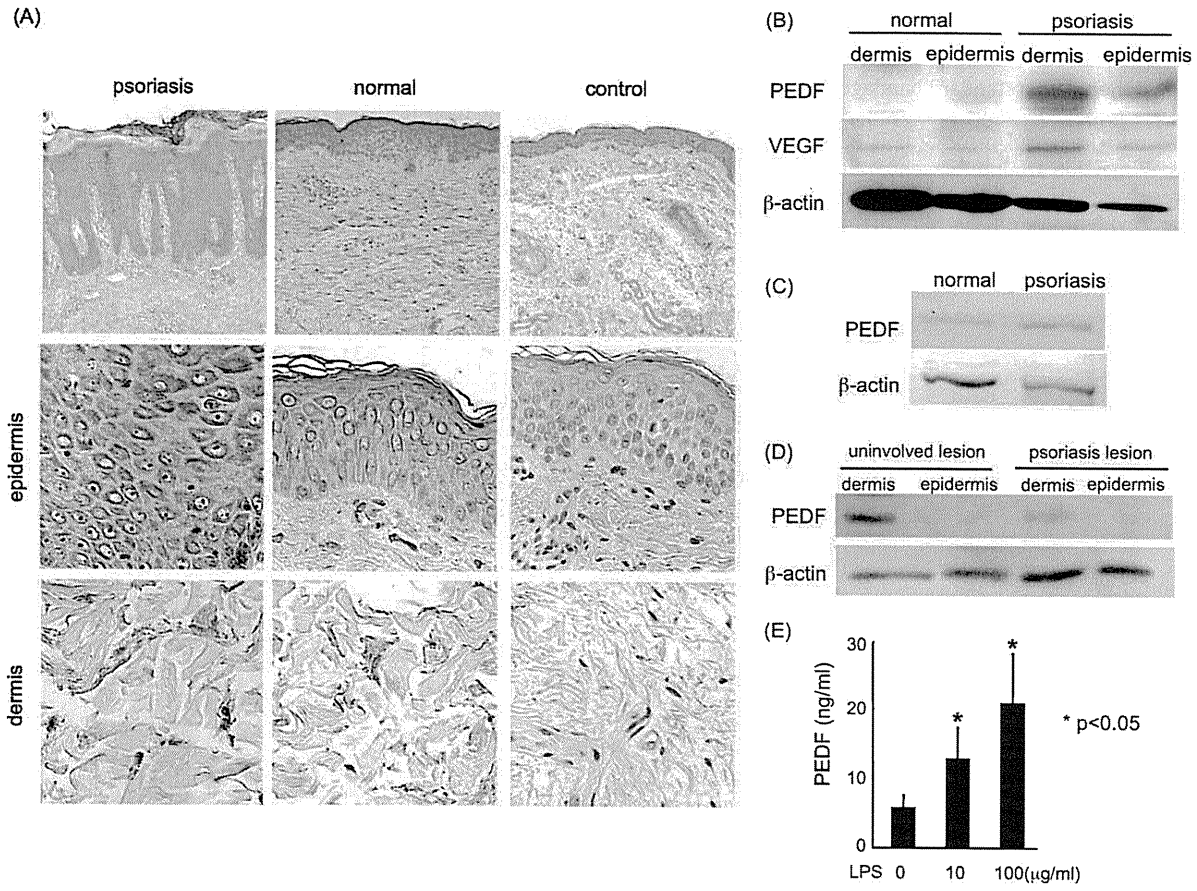

Fig. 1. PEDF is expressed in both the epidermis and dermis. (A) Immunohistochemistry of normal and psoriatic skin lesions. In normal skin, PEDF was detected in both the epidermis and the dermis. PEDF was significantly up-regulated in psoriatic epidermis in comparison with normal epidermis. (B) The expression of PEDF protein was up-regulated in psoriasis lesions. Positive bands were identified with a molecular weight of about 50 kDa from both the epidermis and dermis, which corresponds to the molecular weight of PEDF. (C) PEDF mRNA levels were analyzed using RT-PCR. The expression of PEDF mRNA was slightly up-regulated in psoriasis lesions compared to that of normal skin. (D) The expression of PEDF protein was up-regulated in uninvolved lesion of psoriasis patient compared to psoriasis lesion. (E) The levels of PEDF in the supernatants of cultured normal human keratinocytes were assessed by ELISA. LPS (10 or 100 μg/ml) was used to stimulate keratinocyte production of PEDF ($^*p < 0.05$).

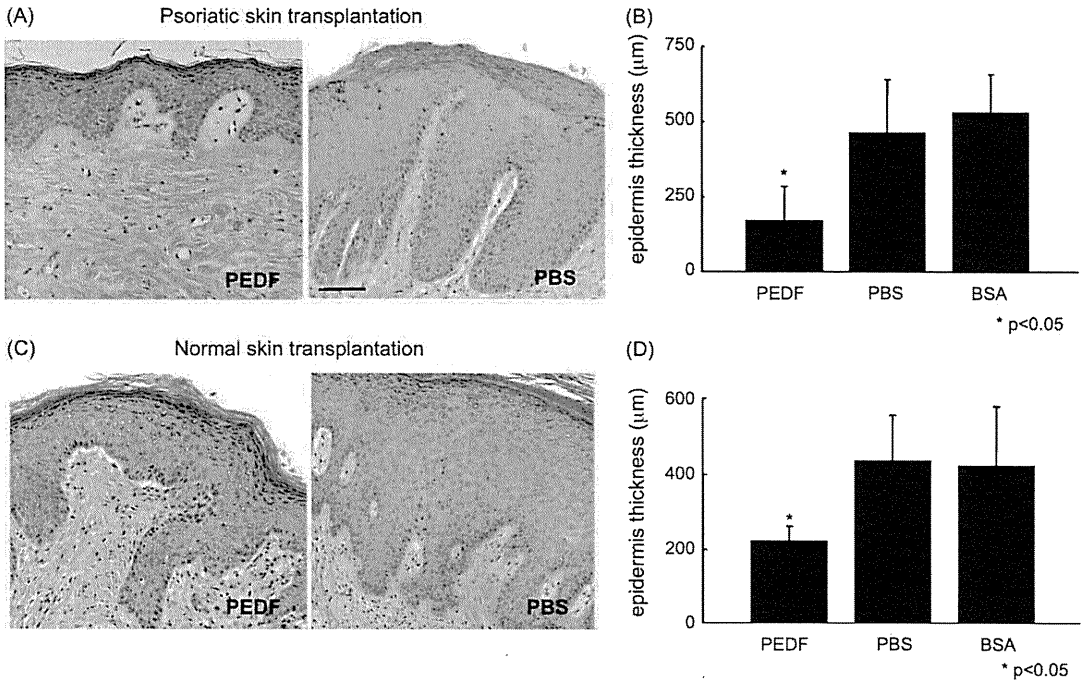

Fig. 2. Intradermal PEDF administration reduced the thickness of grafted epidermis in xenotransplanted SCID mice. Acanthosis was significantly reduced both in psoriatic (A, B) and normal (C, D) skin when compared to PBS or BSA injected groups. Scale bar, 50 μm. Values shown are means and SDs based on four to six measurements per histological section in four histological sections per mouse from duplicate mice transplanted with skin samples from four donors ($^*p < 0.05$).

dressing and then with a standard bandage. Dressing material and sutures were removed 7 days after transplantation.

Grafted mice received recombinant PEDF in 50 μl of PBS by intradermal injection around the xenograft lesion at 30 μg/mouse every three days for three weeks. The PEDF dose was well tolerated without any evident side effects. Mice in the control group received the same volume of PBS or BSA (30 μg). The day after the last injection, biopsies were collected from the transplants from both treatment and control groups. The skin tissues were immediately embedded in OCT reagent and snap-frozen in liquid nitrogen. Cryosections of 5 μm were then prepared for histological and immunohistochemical staining.

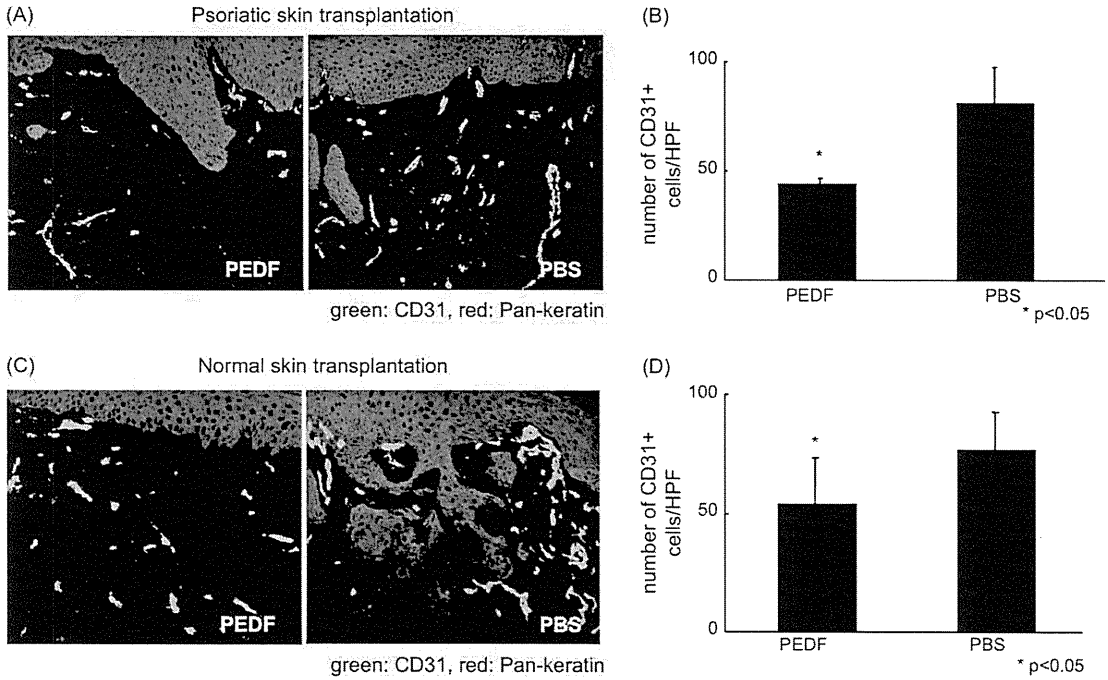

Fig. 3. Intradermal PEDF administration reduced angiogenesis of grafted epidermis. CD31-positive cells (capillary endothelial cells) were enumerated by immunofluorescence after the treatment of psoriatic (A, B) and normal skin (C, D) with PEDF or PBS. Quantification of CD31-positive blood vessels per 100× microscopic field in human skin grafted areas. The data are presented as mean CD31-positive blood vessel numbers per 100× microscopic field, ±SD ($^*p < 0.05$).

2.11. Identification of functional PEDF peptides

Full-length human PEDF cDNA was divided into three parts. Polymerase chain reaction (PCR) products digested by NdeI and SalI were ligated into the multiple cloning site of expression vector pGEX-6P-1 (Amersham Biosciences, Buckinghamshire, United Kingdom). Sequences of the sense and antisense primers were: 5′-AAACATATGCAGGCCCTGGTGCTACTCCTCTGCAT-3′ and 5′-CCCGTCGACTTATGACTTTTCCAGAGGTGCCACAAA-3′ for amplifying F1 cDNA fragment, 5′-AAACATATGTATGGGACCAGGCCCAGAGTCCTGA-3′ and 5′-CCCGTCGACTTAGTCATGAATGAACTCGGAGGTGA-3′ for F2, and 5′-GGGCATATGATAGACCGAGAACTGAAGACCGTGCA-3′ and 5′-AAAGTCGACTTAGGGGCCCCTGGGGTCCAGAAT-3′ for F3. Each human PEDF fragment was purified according to the method of Walker et al. [13]. Human PEDF peptides (see Fig. 6) were synthesized (Sigma–Aldrich, Tokyo, Japan). MG63 human osteosarcoma cells (Health Science Research Resources Bank, Tokyo, Japan) were maintained in Dulbecco's modified Eagle's medium (DMEM) supplemented with 10% of fetal bovine serum (FBS) (ICN Biomedicals Inc., Aurora, OH, USA) and 100 units/ml penicillin/streptomycin. PEDF fragment or peptide treatment was carried out in a medium containing 0.1% of FBS. HUVECs and MG63 cells were treated with or without 100 nM PEDF protein, fragments (F1–F3) or peptides (P1–P6, P5–1, P5–2, and P5–3) or VEGF (25 ng/ml) for 24 h. HUVECs additionally were treated with 100 ng/ml recombinant VEGF (R&D systems) for 2 and 4 days. Cells were incubated with [^{3}H]thymidine (Amersham Bioscience) or 5-bromo-2′deoxyuridine (BrdU) (Roche, Basel, Switzerland) for the last 4 h of culture and proliferation assessed as described previously [14,15].

For the analysis of p21 production, 50 μg of whole cell lysates were prepared and assayed for the expression of p21 and β-actin by Western blotting. Reaction with antibodies and detection with an enhanced chemiluminescence detection system (Amersham Biosciences) were performed as described previously [16].

2.12. Skin penetration of topical applied PEDF peptide

Biotin-labeled PEDF peptide (Sigma–Aldrich) was dissolved in PBS (1 mM) and 70 μl applied to the mouse skin. After 2 h, the applied site was removed and localization in the skin was determined by rhodamine–avidin staining (BD Biosciences). CD31 staining (BD Biosciences) was performed simultaneously and the samples analyzed using a Fluoview confocal laser scanning microscope (Olympus). The experiments of peptide application were repeated 3 times, and 3 mice were used in each experiment.

2.13. Treatment of the grafted psoriatic lesions with PEDF peptide

PEDF peptide was dissolved in PBS (1 mM) and 70 μl of the solution was applied on the grafted site daily for 14 days. No side effects were apparent at the applied sites. Mice in the control group received the same volume of PBS. Biopsies were collected on the day following the last injections and analyzed as described above.

2.14. Statistical analysis

Data were analyzed using unpaired, 2-tailed Student's *t* test. A *p* value less than 0.05 was considered significant.

3. Results

3.1. PEDF is highly expressed in epidermal psoriasis lesions

Immunohistochemical analysis revealed that PEDF protein is present in the cytoplasm of keratinocytes of both psoriatic and normal skin (Fig. 1A). In the dermis, fibroblasts also were positive for PEDF, but the staining was less intense than in the epidermis. Western blotting analysis of human epidermal and dermal proteins revealed a single band with a molecular weight of about 50 kDa (Fig. 1B). PEDF protein and mRNA levels were significantly higher in psoriasis lesions when compared to normal skin (Fig. 1C).

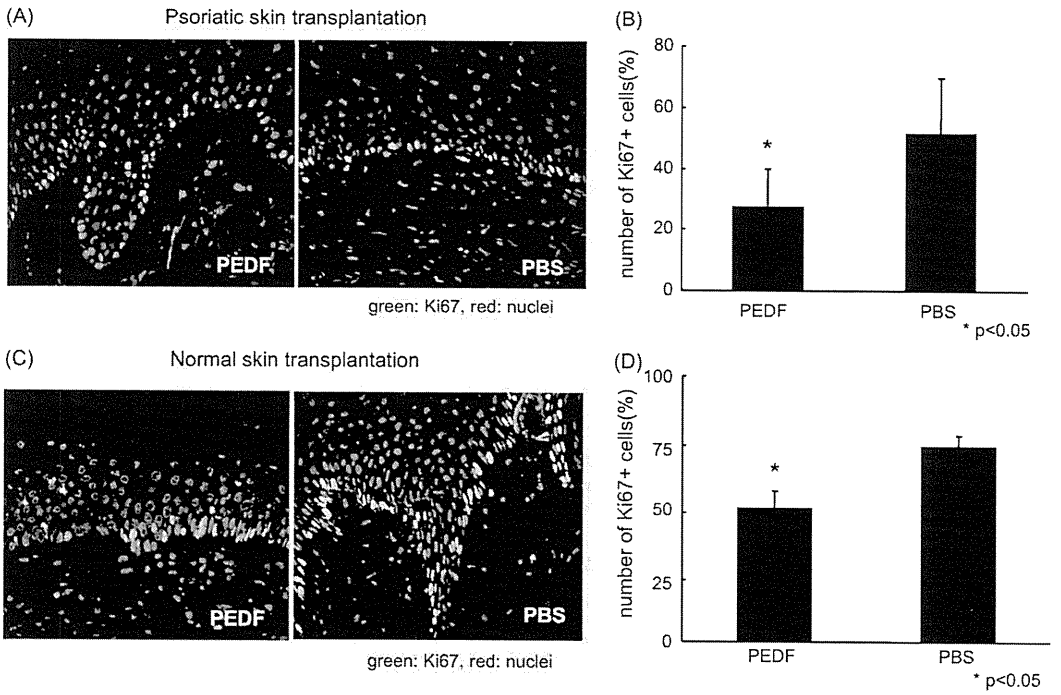

Fig. 4. Epidermal proliferation in basal keratinocytes is inhibited by PEDF. Ki-67-positive (proliferating) cells were stained and enumerated by immunofluorescence after the treatment of psoriatic (A, B) and normal skin (C, D) with PEDF or PBS. The Ki-67-positive keratinocytes in the basal layer were enumerated and the percentage of Ki-67-positive cells in basal layer calculated (*$p < 0.05$).

Interestingly, PEDF protein levels of uninvolved lesion of psoriasis patient were higher than that in psoriasis lesions (Fig. 1D). VEGF also was increased in psoriatic skin, which is consistent with prior reports [6].

3.2. PEDF secretion from cultured keratinocytes after lipopolysaccharide stimulation

PEDF was constitutively secreted by cultured keratinocytes (Fig. 1E) and after LPS stimulation, its secretion was significantly up-regulated in a dose-dependent manner ($p < 0.05$). Fibroblasts by contrast failed to show up-regulation of PEDF secretion after LPS or IL-1β stimulation (data not shown). These results imply that keratinocytes but not fibroblasts secrete PEDF in a regulated fashion in response to inflammatory stimulation. These data contrast with a prior report that PEDF is detected primarily in the dermis, with little protein evident in the epidermal layers [17].

3.3. PEDF levels in serum of psoriasis patients and normal controls

Serum VEGF levels have previously been reported to be significantly elevated in psoriasis patients [6]. If elevated serum VEGF values reflect cytokine overproduction in the skin that then enters the systemic circulation, the pathogenesis in psoriasis might relate not only to a disruption of local angiogenesis in the skin but also to angiogenesis at the systemic level. We next examined whether serum PEDF serum levels also were elevated in psoriasis patients, however we observed no significant difference in PEDF levels between psoriasis patients (14.9 ± 4.1 μg/ml) ($n = 21$) and normal controls (15.1 ± 2.9 μg/ml) ($n = 14$). Furthermore there is no correlation between psoriasis severity and serum PEDF concentration.

3.4. Intradermal injection of PEDF reduces acanthosis, dermal angiogenesis and keratinocyte proliferation of grafted skin by

We hypothesized that PEDF produced by keratinocytes not only regulates local angiogenesis, but also suppresses epidermal proliferation and the resulting acanthosis in psoriatic inflammatory lesions. To investigate this possibility *in vivo*, we studied a psoriasis graft model in which patient-derived skin is xenografted onto severe combined immunodeficient (SCID) mice. Recombinant PEDF (30 μg) was injected intradermally in the area of the graft for three weeks and epidermal thickness evaluated histopathologically. The epidermal thickness of the grafted area was significantly reduced after treatment with PEDF when compared to BSA or PBS treated controls (Fig. 2). Injections of equivalent amounts of BSA, as a non-specific protein control, did not reduce epidermal thickness. Normal human skin transplanted to SCID mice also showed a reduction of epidermal thickness after PEDF-treatment. On the

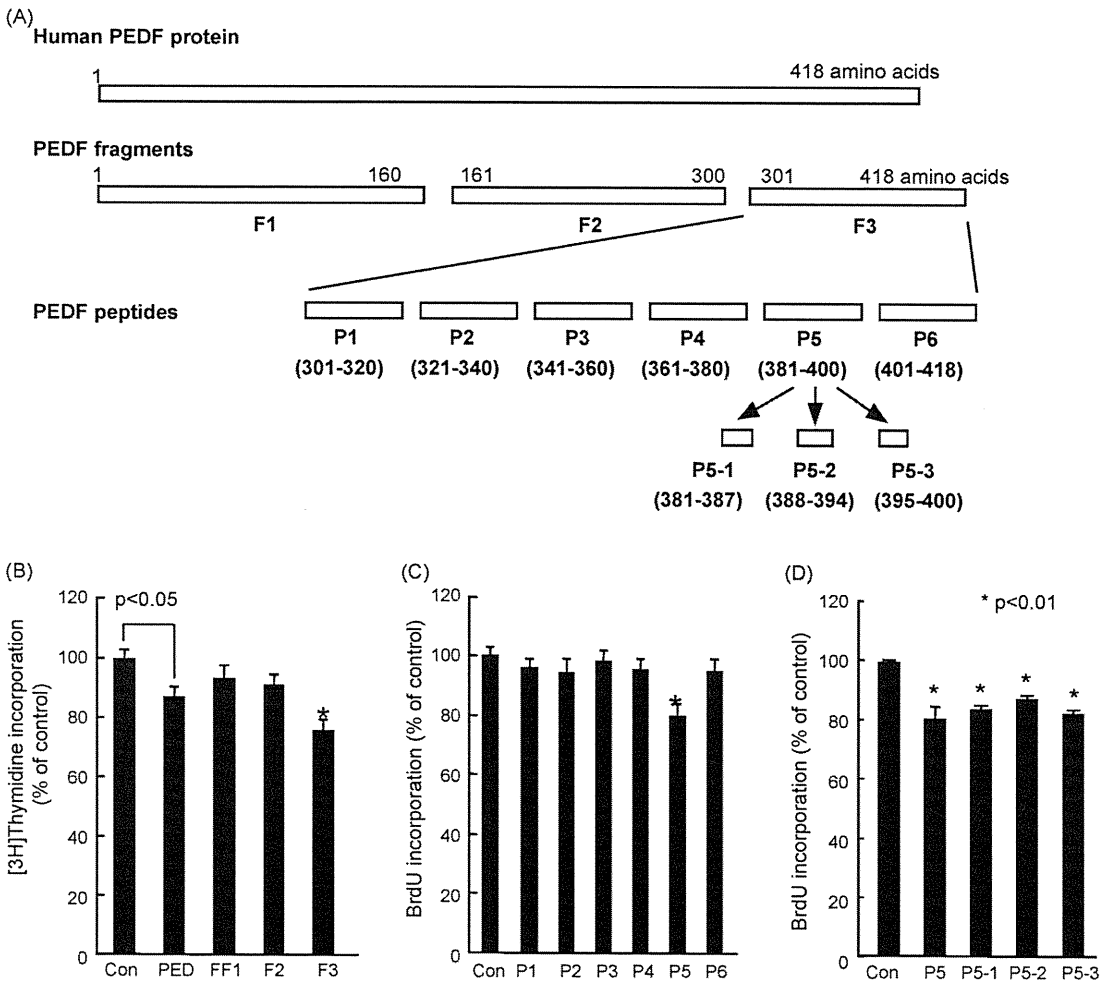

Fig. 5. Anti-angiogeneic activity of PEDF peptides. Diagram of the PEDF peptides studied for their effect on the growth of MG63 cells (B–D) or HUVEC (E). MG63 cells or HUVEC were treated with or without 100 nM PEDF, fragments or peptides and then [^{3}H]thymidine (B) and BrdU incorporation into the cells (C, D) were measured. The percentage of [^{3}H]thymidine or BrdU incorporation is indicated on the ordinate and related to the value of the control. *$p < 0.01$ compared to the value with 100 nM PEDF protein.